WL-TR-91-4109

X-RAY COMPUTED TOMOGRAPHY FOR WHOLE SYSTEM EVALUATION (SMALL JET ENGINES)

Alan R. Crews
Richard H. Bossi

Boeing Defense & Space Group
P.O. Box 3999
Seattle, WA 98124

May 1992

Interim Report for Period June 1990 to February 1991

MATERIALS DIRECTORATE
WRIGHT LABORATORY
AIR FORCE SYSTEMS COMMAND
WRIGHT-PATTERSON AIR FORCE BASE, OHIO 45433-6533

NOTICE

When Government drawings, specifications, or other data are used for any purpose other than in connection with a definitely Government-related procurement, the United States Government incurs no responsibility or any obligation whatsoever. The fact that the government may have formulated or in any way supplied the said drawings, specifications, or other data , is not to be regarded by implication, or otherwise in any manner construed, as licensing the holder, or any other person or corporation: or as conveying any rights or permission to manufacture, use, or sell any patented invention that may in any way be related thereto.

This report is releasable to the National Technical Information Service (NTIS). At NTIS, it will be available to the general public, including foreign nations.

This technical report has been reviewed and is approved for publication.

Charles F. Buynak

CHARLES F. BUYNAK
Nondestructive Evaluation Branch
Metals and Ceramics Division

TOBEY M. CORDELL, Chief
Nondestructive Evaluation Branch
Metals and Ceramics Division

FOR THE COMMANDER

Norman M Tallan

DR NORMAN M. TALLAN, Director
Metals and Ceramics Division
Materials Directorate

If your address has changed, if you wish to be removed from our mailing list, or if the addressee is no longer employed by your organization please notify WL/MLLP , WPAFB, OH 45433-6533 to help us maintain a current mailing list.

Copies of this report should not be returned unless return is required by security considerations, contractual obligations, or notice on a specific document.

REPORT DOCUMENTATION PAGE

Form Approved
OMB No. 0704-0188

1. AGENCY USE ONLY (Leave Blank)	2. REPORT DATE	3. REPORT TYPE AND DATES COVERED
	MAY 31, 1992	Interim/ Jun 90 - Feb 91

4. TITLE AND SUBTITLE

X-Ray Computed Tomography for Whole System Evaluation (Small Jet Engines)

5. FUNDING NUMBERS

F33615-88-C-5404
PE: 63112F
PR: 3153
TA: 00
WU: 06

6. AUTHOR(S)

Alan R. Crews and Richard H. Bossi

7. PERFORMING ORGANIZATION NAME(S) AND ADDRESS(ES)

Boeing Defense & Space Group
P.O. Box 3999
Seattle, WA 98124-2499

8. PERFORMING ORGANIZATION REPORT NUMBER

9. SPONSORING/MONITORING AGENCY NAME(S) AND ADDRESS(ES)

Charles F. Buynak (513)255-9802
Materials Directorate (WL/MLLP)
Wright Laboratory
Wright-Patterson AFB, OH 45433-6533

10. SPONSORING/MONITORING AGENCY REPORT NUMBER

WL-TR-91-4109

11. SUPPLEMENTARY NOTES

12a. DISTRIBUTION/AVAILABILITY STATEMENT

Approved for public release; Distribution is unlimited

12b. DISTRIBUTION CODE

13. ABSTRACT (Maximum 200 words)

Under a preliminary testing task assignment of the Advanced Development of X-Ray Computed Tomography Application program, computed tomography (CT) has been studied for its potential as an engineering analysis tool and an in-service nondestructive evaluation method for whole systems such as small jet engines. CT evaluation has been employed on small jet engines demonstrating its viability for assembly verification, dimensional profiles, and foreign object detection without disassembly. CT systems with energies of 400 kV, 2 MV, 2.5 MV and 9 MV were used in the study. The sensitivity to feature details in complex systems, such as the jet engines, is improved with higher signal to noise for the same inherent resolution. For long metal paths, the highest energy available is preferred, however many of the 2 MV images showed good sensitivity to internal details, and even 400 kV can be usefully employed in some regions of an engine.

The quantitative capability of CT to measure the relative X-ray linear attenuation coefficient and position of small volume elements in an object offers the potential to directly calculate the center-of-gravity (CG) of the object from the CT scan data. Results of CT tests on a test phantom indicates that under certain conditions CG calculations can be made for CT data with sensitivity on the order of 0.15 g-cm in aluminum at 3 cm radius. However, the application of the CT technique to internal rotating component balancing in a whole system involves consideration of the shape of the rotating hardware and the effect of surrounding material, which has been found to seriously distort results.

14. SUBJECT TERMS		15. NUMBER OF PAGES
Computed Tomography (CT)	Density	50
Air Launched Cruise Missile (ALCM)	Jet Engine	
Center-of-Gravity (CG)	Foreign Object Detection	16. PRICE CODE
	Nondestructive Eval/Inspection(NDE/I)	

17. SECURITY CLASSIFICATION OF REPORT	18. SECURITY CLASSIFICATION OF THIS PAGE	19. SECURITY CLASSIFICATION OF ABSTRACT	20. LIMITATION OF ABSTRACT
Unclassified	Unclassified	Unclassified	UL

NSN 7540-01-280-5500

Standard Form 298 (Rev. 2-89)
Prescribed by ANSI Std. Z39-18
298-102

TABLE OF CONTENTS

APPENDICES

LIST OF FIGURES

LIST OF TABLES

SUMMARY

Computed tomography (CT) scanning has been performed on small jet engines, demonstrating its viability for assembly verification, dimensional profiles, and foreign object detection without disassembly for whole system evaluation. Regions of interest evaluated in the engines included the compressor stages, stators, burner/combustor, labyrinth seals and turbines. The sensitivity to feature details in complex systems is a function of the inherent resolution, signal to noise and energy of the CT scanning conditions. The ability to be sensitive to internal details generally increased with the CT system energies used from 400 kV to 2 MV to 9 MV. For long metal paths the highest energy available is preferred, however many of the 2 MV images showed good sensitivity to internal details, and even 400 kV can be usefully employed in some regions of an engine.

The quantitative capability of CT to measure the relative X-ray linear attenuation coefficient and position of small volume elements in an object offers the potential to directly calculate the center-of-gravity (CG) of the object from the CT scan data. Results of tests on a simple test phantom indicates that CT can be sensitive to better than 0.15 g-cm in aluminum at 3 cm radius. This is in the range of accuracy used in dynamic balancing of small jet engine components, however, the CT measurements are sensitive to the test conditions and the data processing. For example, the application of the CT technique to internal rotating component balancing in a whole system involves consideration of the effect of surrounding material, which has been found to seriously distort results. Also, the three dimensional shape of actual rotating hardware in an engine is different from the idealized phantom and was not evaluated in this study. While CT was found to be very sensitive to changes in CG, different data processing schemes were found to result in offset differences in the absolute CG measurement position. The use of a comparison of CG measurements from CT scans at two or more positions of the rotating assembly can be used compensate for these offsets in determining the balance and should also minimize the effect of the outside static structure.

ACKNOWLEDGEMENTS

The authors extend special thanks to the Air Force Oklahoma City, Air Logistic Center and Teledyne CAE, Toledo, Ohio for the loan of small jet engines for testing. We also acknowledge the assistance of ARACOR, Hill AFB, Rocketdyne, BIR and NASA for CT imaging of the engines. Special thanks are due to Cindy Berglund, John Cline, Jud Geiger, Gary Georgeson and Jim Nelson of Boeing for their efforts on this task assignment.

DISCLAIMER

The information contained in this document is neither an endorsement nor criticism for any X-ray imaging instrumentation or equipment used in this study.

1.0 INTRODUCTION

The goal of the Advanced Development of X-Ray Computed Tomography Applications demonstration (CTAD) program is to evaluate inspection applications for which X-ray computed tomography (CT) can provide a cost-effective means of evaluating aircraft/aerospace components. The program is "task assigned" so that specific CT applications or application areas can be addressed in separate projects. Three categories of task assignments are employed in the program: 1) preliminary tests where a variety of parts and components in an application area are evaluated for their suitability to CT examinations; 2) final tests, where one or a few components are selected for detailed testing of CT capability to detect and quantify defects; and 3) demonstrations, where the economic viability of CT to the inspection problem are analyzed and the results presented to government and industry. This interim report is the result of a preliminary task assignment study on whole systems. Additional task assignment reports previously issued by the CTAD program are listed in references 1 through 8.

1.1 Computed Tomography

X-ray computed tomography (CT) is a powerful nondestructive evaluation technique that was conceived in the early 1960's and has been developing rapidly ever since. CT uses measurements of X-ray transmission from many angles about a component to compute the relative X-ray linear attenuation coefficient of small volume elements and presents them as a cross sectional image map. The clear images of an interior plane of an object are achieved without the confusion of superposition of features often found with conventional film radiography. CT can provide quantitative information about the density/constituents and dimensions of the features imaged. Appendix A compares the basic radiographic (RT), digital radiography (DR) and CT techniques utilized in the CTAD program.

Although CT has been predominantly applied to medical diagnosis, industrial applications have been growing over the past decade. Medical systems are designed for high throughput and low dosages specifically for humans and human sized objects. These systems can be applied to industrial objects that have low atomic number and are less than one-half meter in diameter. Industrial CT systems do not have these dosage and size constraints. They are built in a wide range of sizes from the inspection of small jet engine turbine blades using mid-energy (hundreds of kV) X-ray sources to the inspection of large ICBM missiles requiring high (MV level) X-ray energies. The high energy industrial CT systems provide the penetration capability necessary to evaluate complex systems containing metallic components, such as small jet engines.

1.2 Scope and Objective

This task assignment, designated "Task 8 - Whole Systems", is a preliminary testing task directed at the technical and economic viability of CT as an assembly verification, failure analysis and in-service evaluation method for small jet engines. Engines are a complex assembly of subcomponents that have significant material and structure variations. As such, the results of the engines measurements allow the extrapolation of CT benefits to many other systems that are similar in complexity.

Specific objectives include the determination of CT system requirements for assembly verification, dimensional profiles, foreign object detection, corrosion detection and seal integrity in the compressor stages. The CT system X-ray energy required for sufficient penetration and feature sensitivity in the engine is of particular interest. Because CT provides quantitative

measurement of X-ray linear attenuation coefficient and position in small volumetric units throughout a cross section of a component, the data can be used to estimate the center-of-gravity (CG) of a component or a combination of components. The potential of this capability for rotating components is addressed in this study.

A specific goal for the CG measurements is a preliminary assessment of applicability for estimating small jet engine balance. The simple test phantom for CT measurements of CG was scaled to the diameter of small jet engines. The measurement accuracy was compared to the requirements of current engine rotating component dynamic balance practice.

2.0 TEST PLAN

The Preliminary Testing of the engine measurements involved the acquisition of test components, development of a CG algorithm, CT scanning, data evaluation, preliminary economic assessment, development of Final Testing plans and reporting.

2.1 Part Acquisition

The primary whole system test items for this task assignment were small jet engines: a Williams model F107-WR-400 Tomahawk Cruise Missile Engine (CME), a Teledyne J402 model 373 helicopter drone engine, and a damaged ALCM CME. Table 2.1-1 lists the engines.

Table 2.1-1 Small Jet Engines

PID#	Engine Model (manufacturer)	Size	Weight	Application
080107	F107-WR-400 CME (Williams)	96 cm X 46 cm	67 kg	Tomahawk
080105	J402 (Teledyne)	85 cm X 32 cm	63 kg	Helicopter Drone
080106	F107-WR-101 CME	109 cm X 36 cm	71 kg	ALCM

In order to address the potential of CT to calculate center of gravity (CG) of a component, a test phantom consisting of an aluminum disk with a raised lip and center bushings of aluminum were manufactured, in configurations where the CG could be analytically determined. The disk is 30 cm (12 inch) in diameter to correspond to the size of typical small engine versions. Figure 2.1-1 shows the CG disk test phantom with two bushings placed on the disk for photography. Figure 2.1-2 is a schematic drawing of the phantom. The aluminum bushing mounts in a groove in the disk. Three bushings were fabricated. One was complete, one had 0.5 g of material removed (ground flat off of the bushing edge) and a third had 1.0 g of material removed.

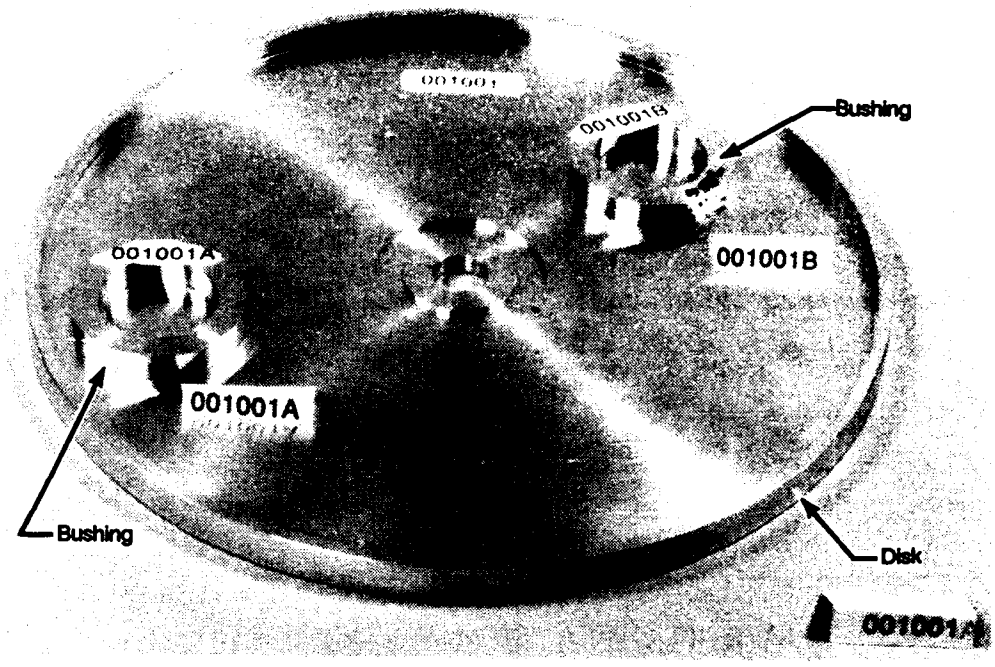

Figure 2.1-1 Photograph of the CG disk test phantom.

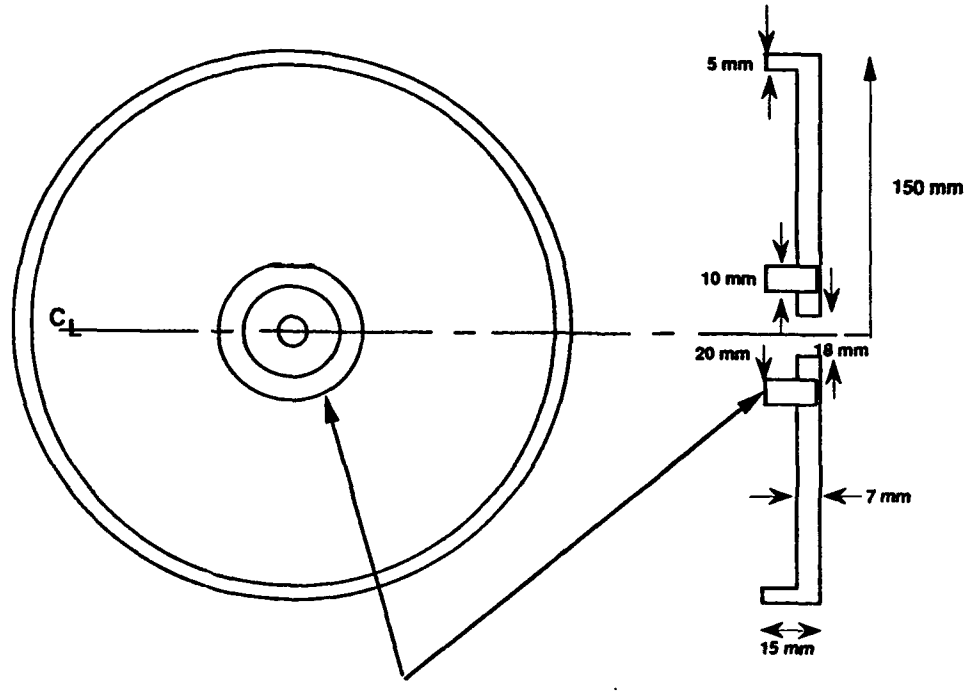

Figure 2.1-2 Schematic of the CG disk test phantom.

This test phantom was designed to have at least some similarity to a CME internal rotating hardware. Presently, balancing of the internal components of a CME at Oklahoma City Air Logistics Center (OC-ALC) is performed by using a dynamic balance and grinding of the component at the proper orientation for selective weight removal. The typical procedure performs the grinding at a radius of 3 cm (1.2 inch). The balancing activity is performed until the weight tolerance is 0.28 g. The test phantom was consequently designed so that the removal of material at the bushing radius of 3 cm represents the typical position of grinding for the balancing of CME compressor and turbine engine parts at the OC-ALC. The raised lip and center bushing can be imaged as two concentric rings when a CT slice is taken just above the plane of the disk portion of the phantom.

The phantom is intentionally much simpler than an engine disk to allow testing of the CG measurement concept. The ring of material at the outside provides uniform mass for modelling rather than a number of shaped blades in an engine. Also, aluminum was used instead of a nickel alloy, to allow the use of lower energy CT systems for penetration. The density is therefore about one-third of the density of engine components.

2.2 CT Testing

CT testing at appropriate facilities was based on the availability of CT systems capable of handling the test objects. For the engine scans four CT systems having different energies of 400 kV, 2 MV, 2.5 MV and 9 MV were used. The different energy levels provide a test of the necessary X-ray penetration capability for adequate evaluation of the engines. For the CG measurement on the test phantom the scanning was performed on two different designs of 400 kV systems and a 9 MV system.

CT operating parameters such as slice width and scan time were chosen based on the normal procedures used for items typical of the engines on each system. The sensitivity of the CT systems were measured using test phantoms developed for the CTAD program described in Appendix B. Table 2.2-1 lists some of the operating parameters of the CT systems. All the systems had adequate modulation at 1 lp/mm but could not resolve 2 lp/mm. The signal to noise ratio (S/N) varied considerably depending on the slice thickness, energy, scan time and field of reconstruction. In general S/N in the aluminum test phantom varies from 10 for system S at 1 mm slice thickness to near 100 for systems H and U at 4 mm slice thickness.

The data from the CT scanning at the various facilities was stored on tape and processed at Boeing. The images of the engines are best observed on an image processing workstation monitor where the contrast can be optimized for regions of interest and zoom can be used for reviewing details in the relatively large components. Hardcopies have been generated for this report, however printing and reproduction severely limit the quality of detail in the report figures, particularly for the large area images. In a few cases photographs taken from a workstation monitor were reproduced. Readers are cautioned that the reproduced report images do not reflect the true sensitivity available in the original CT data.

Table 2.2-1 CT Systems					
			Typical Operation		
System	Energy (kV)	Max. Part Diameter (m)	Slice Thickness (mm)	Scan Time (min)	Field of Reconstruction (mm)
A	400	0.8	2	25	300
L	400	1.8	4	12	300
H	2000	1.5	4	5	600
S	2500	1.5	1	28	600
U	9000	1.5	5	5	600

2.3 Data Evaluation

Data evaluation of the engine scans primarily consisted of the assessment of the detectability of various features within the engines. The images from the four different energy CT systems at were reviewed for the visual detail in the CT image to perform assembly verification, assess static structure condition, determine dimensional profiles, detect foreign objects and evaluate bearing assemblies and seals. Table 2.3-1 lists the evaluation criteria.

Table 2.3-1 Evaluation Criteria of CT Images on Engines	
Criteria	Details of Interest
visibility of features	recognition of features adequate separation of detail
material sensitivity	variation of materials detection of voids/inclusions
drawing verification	comparison of CT to drawing

Data evaluation of the CG disk test phantom was performed using software developed to calculate CG by two different approaches. Evaluation of CG measurements on actual engines or engine component was not performed during this task assignment. Only the test phantom CG accuracy was evaluated.

3.0 ENGINE EVALUATION

3.1 Engine Maintenance

The maintenance of small jet engines requires a periodic complete overhaul to evaluate the internal conditions. The specific overhaul operations are: remove auxiliary components, disassemble main engine, disbond parts, clean or strip parts, machine parts as necessary, perform visual and physical inspection, perform measurements, perform nondestructive inspection, balance individual parts, balance assemblies, perform finish machining, replace aged or unacceptable parts, bond parts together, seal assemblies, finish mechanical assembly, and power test. These activities require the expenditure of material resources (including some hazardous materials and chemicals) and increase the risk of component damage during handling. There are age sensitive components such as seals and grease packed bearings which must be replaced at well defined intervals and require disassembly, but the majority of the actions at intermediate times are basically inspection issues.

Overhaul of CME engines is a maintenance function of the Air Force, Oklahoma City Air Logistics Center (OC-ALC). Current procedures for a typical CME overhaul requires nearly 100 hours of labor. The overhaul will occur on a periodic schedule which requires either partial or complete disassembly. These small jet engines, maintained at the Air Force OC-ALC, have an approximate four year partial breakdown cycle and eight year complete overhaul cycle. Any process which could reduce or eliminate the breakdown activity while providing an adequate evaluation of the engine condition is desirable, saving resources, avoiding environmentally sensitive hazardous material use and disposal, and reducing risk to personnel and damage of equipment.

3.2 CT Scanning Results

3.2.1 F107-WR-400 Engine

The F107 engines are used on the Sea, Ground and Air Launched Cruise Missiles. The -400 series is used on the Sea and Ground launched versions. The F107-WR-400 Cruise Missile Engine (CME) is a nonaugmented, twin spool, axial flow turbofan engine with a mixed exhaust. Figure 3.2-1 is a photograph of the CME including the accessory packages. Figure 3.2-2 is an isometric exploded drawing of the engine. The low pressure spool consists of a two stage axial fan followed by two additional axial compressor stages in the gas generator flow path, these are all driven by two axial turbines. The high pressure spool consists of a single stage centrifugal compressor driven by a single axial turbine The shafts are counter-rotating to minimize gyroscope and shaft vibration effects. The engines use a folded annular burner with rotary fuel injection. It provides a maximum of 600 pounds of thrust and is approximately 97 cm (38 inches) long, 46 cm (18 inches) wide, 43 cm (17 inches) high and weighs 67 kg (148 pounds).

The F107 CME was CT scanned on four different CT systems, at X-ray energies of 420 kV, 2 MV, 2.5 MV and 9 MV. The purpose of scanning on the different energy systems was to evaluate the minimum energy required to provide adequate detail information. CT scans were taken across the main axis of the engine to reveal details of compressor stages, stators, burner/combustor and seals. The 2 MV and higher energy systems also had sufficient penetration capability to allow longitudinal CT scans of the engine while in the shipping container.

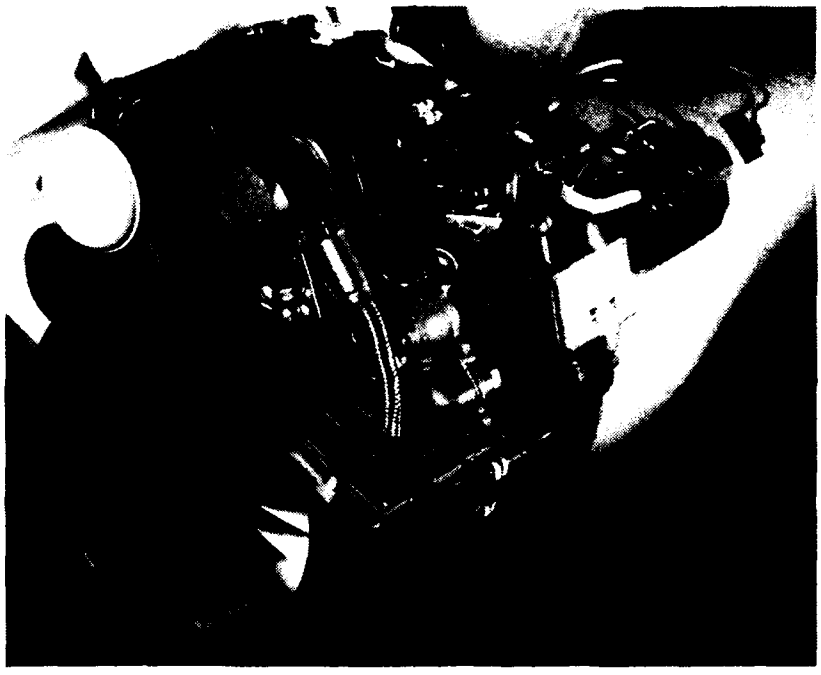

Figure 3.2-1 Photograph of the F107-WR-400 CME.

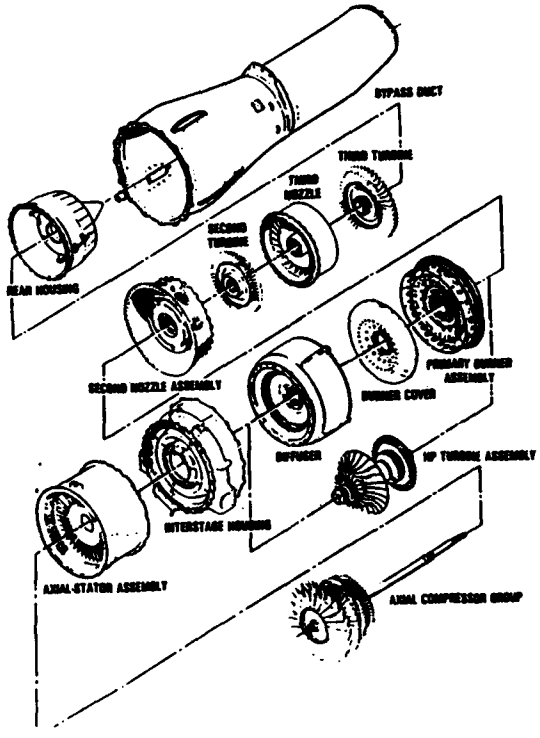

Figure 3.2-2 Isometric exploded drawing of the F107 CME engine assembly.

Figure 3.2-3 shows the CME being mounted on the turntable of a 2.5 MV CT system. The straps were removed and the shipping container was secured to the CT system table before scanning. The fact that the unit can be inspected in many instances without being unpacked or specially fixtured is a unique advantage of X-ray in general and CT in particular. This advantage provides time, safety (part and personnel) and cost savings.

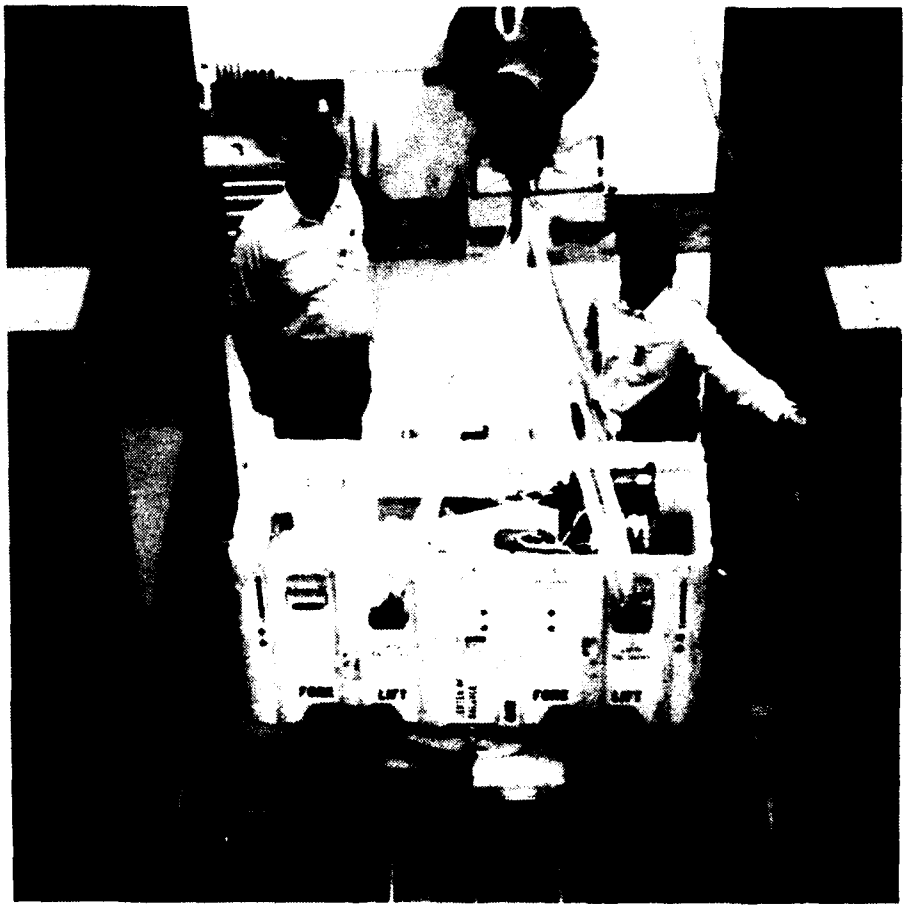

Figure 3.2-3 Mounting the F107 engine on a 2.5 MV CT system (System S). Hank Scudder and Jeff Anders of Rocketdyne are present.

Figure 3.2-4 is a digital radiograph of the CME taken on a 2.5 MV CT system. The digital radiograph has sufficient penetration for the engine materials and good resolution to detail. The dynamic range of a digital detector array allows the entire engine to be evaluated from the data set. However, the complexity of the engine results in a superposition of detail that limits the useful information that can be obtained from radiographic imaging.

Digital radiography, as part of the evaluation capability of CT systems, does provide a preliminary overall review of a system. From the digital radiograph, the mid-plane longitudinal location (axis) of the engine on the CT system can be establish for CT examination.

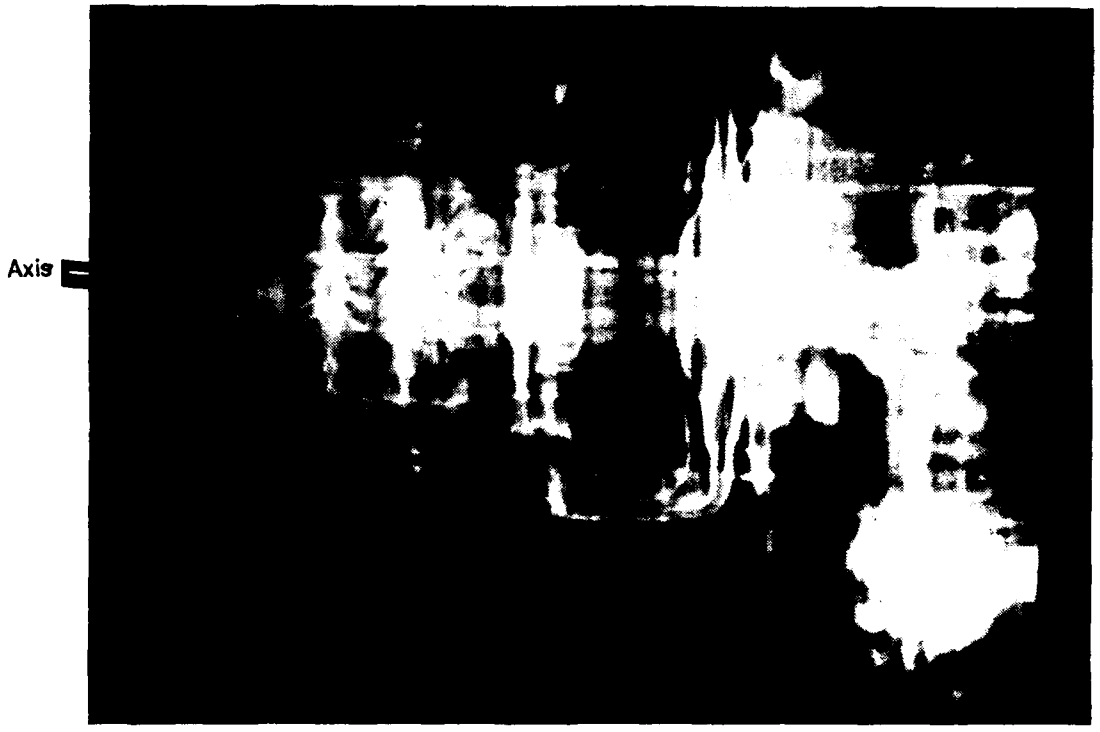

Figure 3.2-4 Digital radiograph of the F107 engine on a 2.5 MV CT system (System S).

Figure 3.2-5 shows a mid-plane longitudinal CT scan of the CME taken on a 2.5 MV CT system. All of the compressor and turbine stages are clearly visible, with the actual blades partial volumed due to their angulation relative to the CT image plane. The burner area and the labyrinth seal are clearly distinguishable although the fuel slinger is not. The centrifugal compressor shows signs of photon starvation due to its size, material and configuration. The central shaft portion shows a combination of photon starvation and edge artifacts to the point where it can not be clearly distinguished at some places. This results from both the long path lengths of high density material and the straight edges of the hollow shaft. The signal to noise ratio is relatively low in this image due to a thin (1 mm) slice width and the scanner design/operating regime. The thin CT slice does provide a good definition of the walls of the engine structures.

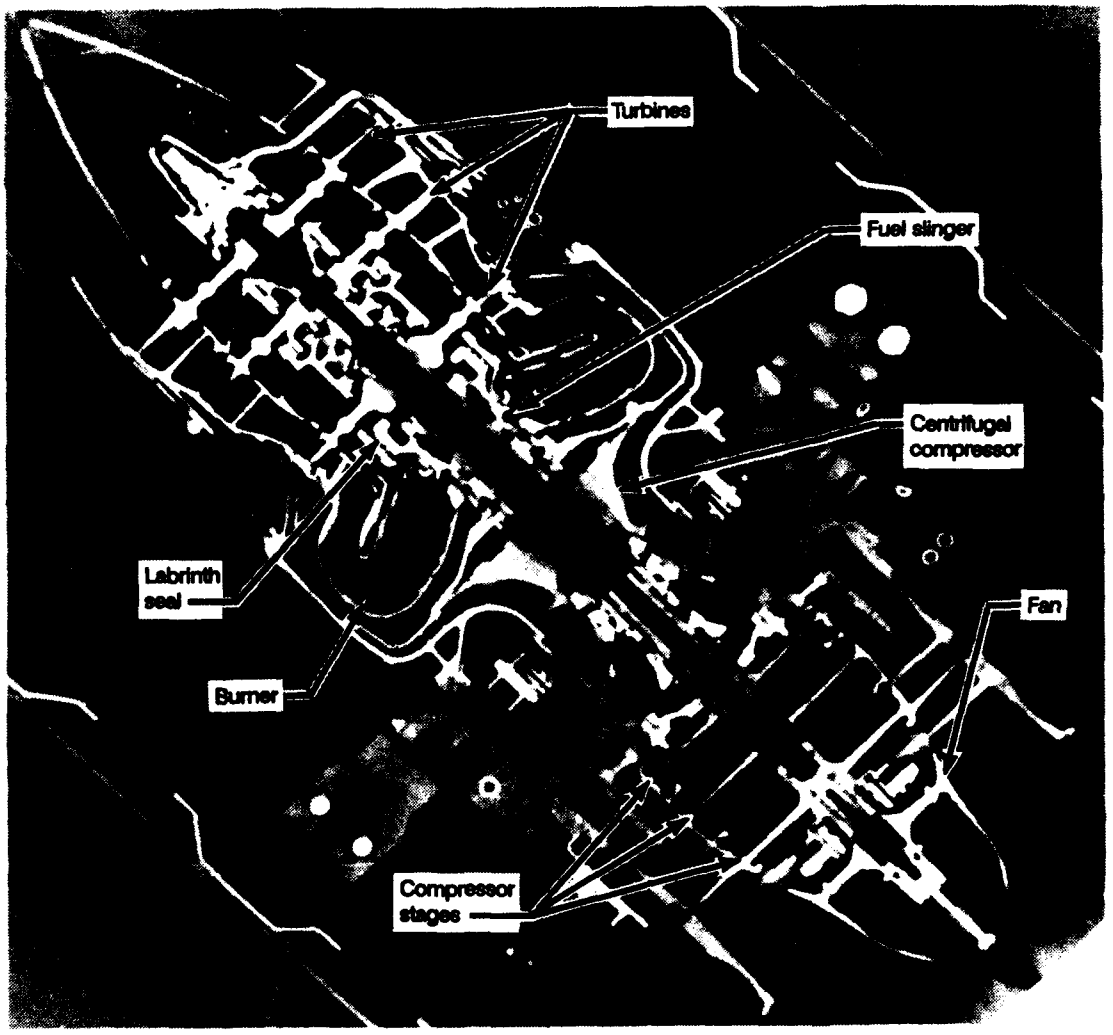

Figure 3.2-5 Mid-plane longitudinal CT slice of the F107 engine on a 2.5 MV CT system (System S).

Figure 3.2-6 shows a mid-plane longitudinal CT scan of the CME taken on a 2 MV CT system. Again, all of the compressor and turbine stages are clearly visible as well as the burner area and the labyrinth seal. The photon starvation along the long path lengths and edge artifacts are not quite as severe in this data as in the Figure 3.2-5 data. The signal to noise ratio is higher in this figure than the previous, primarily due to a thicker CT slice (5 mm) and differences in the number of detectors and views used in the data detection and image reconstruction. The thicker slice does risk blurring of structure walls on cylindrical objects.

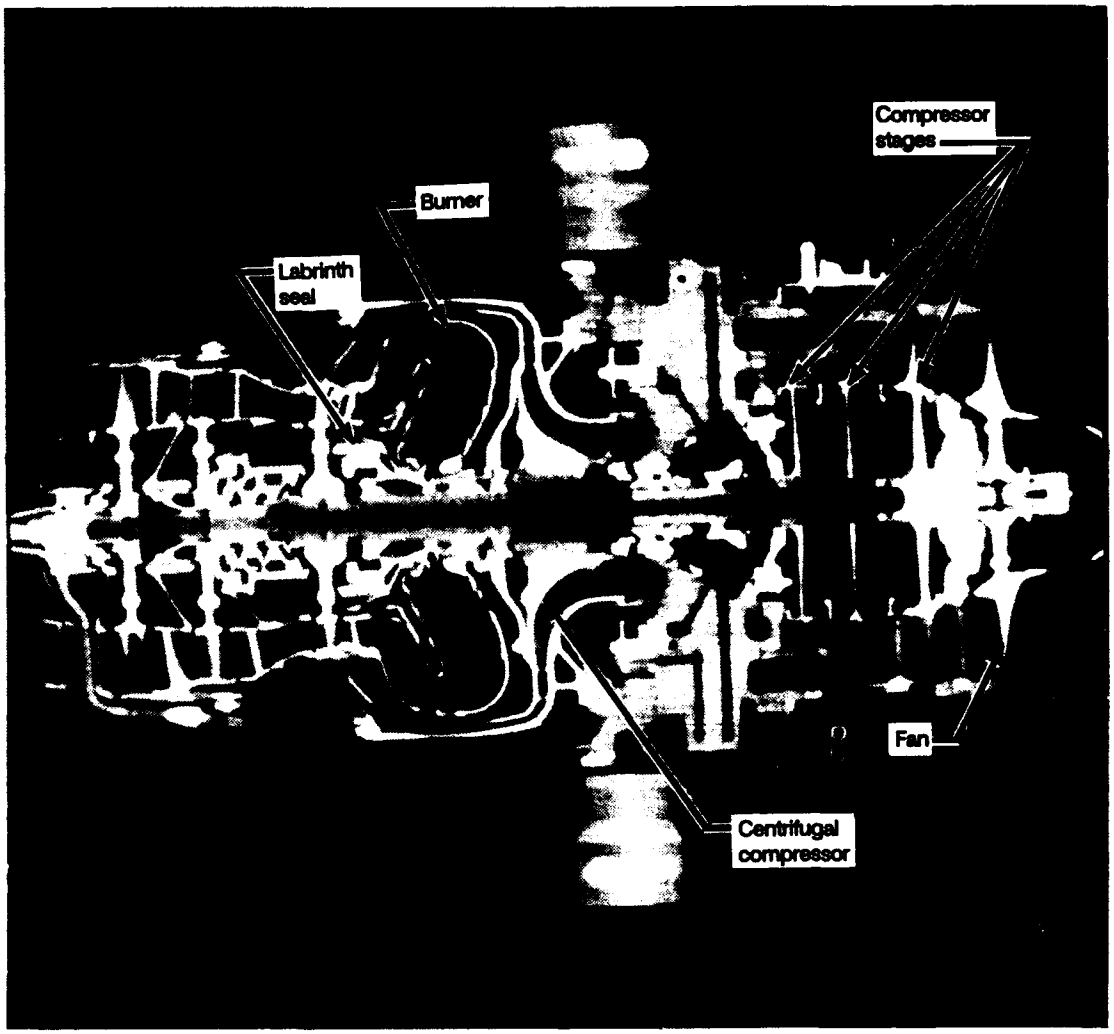

Figure 3.2-6 Mid-plane longitudinal CT slice of the F107 engine on a 2 MV CT system (System H).

Figure 3.2-7 shows the mid-plane longitudinal CT scan of the CME taken on a 9 MV CT system. In the CT slice, the compressor and turbine stages are clearly visible along with the burner area and labyrinth seal. The central shaft and centrifugal compressor show less photon starvation than the thin slice 2.5 MV image (Figure 3.2-5). The thick slice 2 MV image (Figure 3.2-6) and the 9 MV image are comparable, however there is a slightly higher signal to noise in the 9 MV image attributed to the higher energy. Image quality along the long central shaft benefits from the high (9 MV) energy imaging.

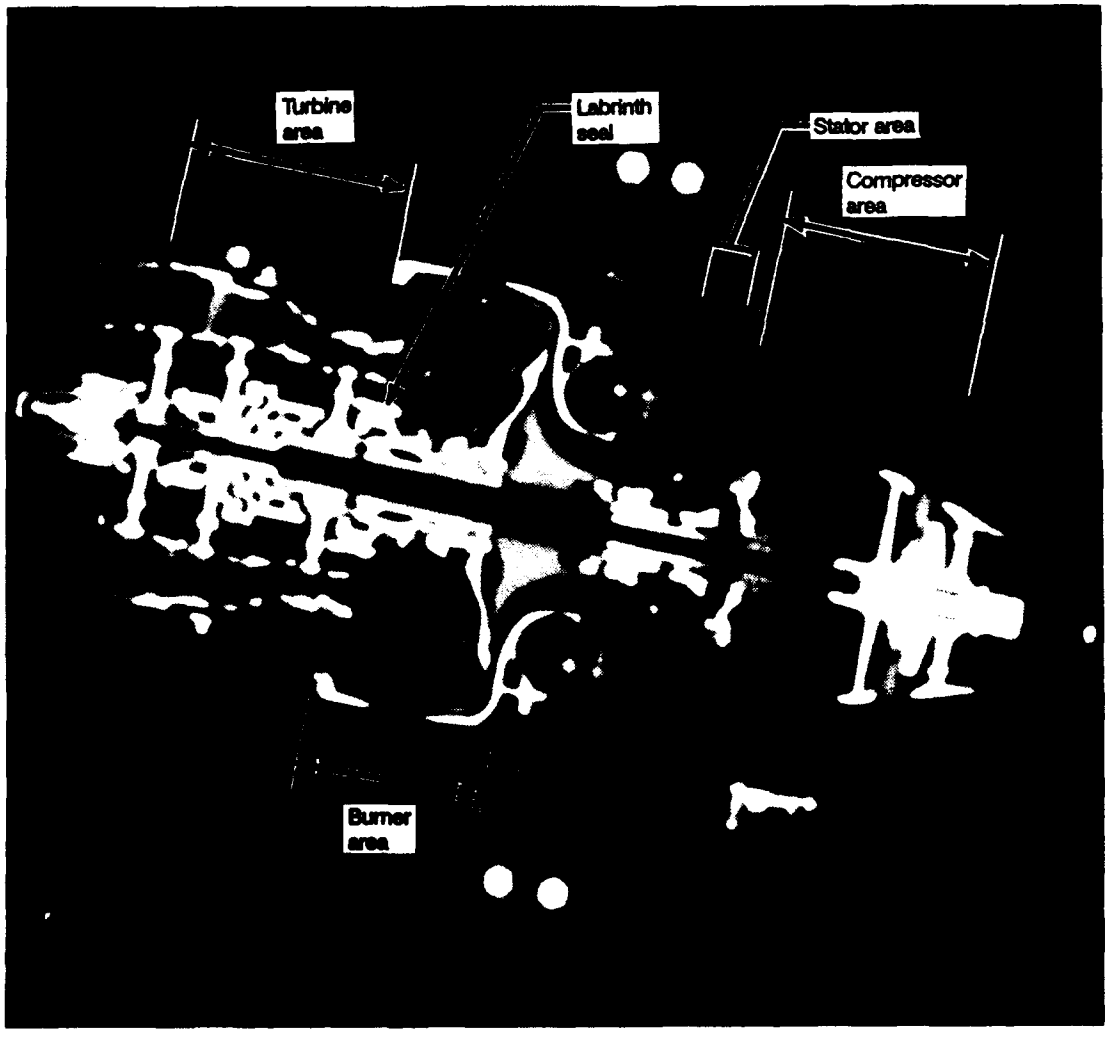

Figure 3.2-7 F107 engine mid-plane longitudinal CT slice on a 9 MV CT system (System U).

The longitudinal slices provide dramatic images of the CME assembly configuration. Although 2 MV images are adequate for major feature detection, there is some photon starvation along certain paths that is more severe than with the 9 MV system. The relative resolution of the systems appears to be approximately equivalent for observing details such as the labyrinth seal. Resolution is limited to high contrast features of approximately 0.5 mm in size.

CT slices across the engine were taken at five areas of interest indicated in Figure 3.2-7. The first area of interest is the compressor stages. Figure 3.2-8 is a CT slice of the 1st axial compressor from the 400 kV system. The image has sufficient sensitivity to detect a "nick" in a blade which has been feathered out. Figure 3.2-9 is a CT slice from a 2.5 MV system, with a thin (1 mm) slice width, also taken through the 1st axial compressor and shows the "nick", although the compressor has rotated. The 9 MV CT slice of Figure 3.2-10 through the same compressor stage does not show the "nick" because it has not been taken at the same specific axial location. Figures 3.2-11 through 3.2-14 are CT slices in the second axial compressor stage from the 400 kV, 2.5 MV with thin slice, 2 MV with thicker slice and 9 MV systems respectively. The slices show the turbine blade assembly. Again, the slices are not specifically at the same height from the three CT systems. These images indicate that the resolution of the systems is approximately the same, the detail sensitivity improves with the X-ray energy. The thick slice 2 MV and 9 MV systems show the least amount of artifacting and the greatest signal to noise.

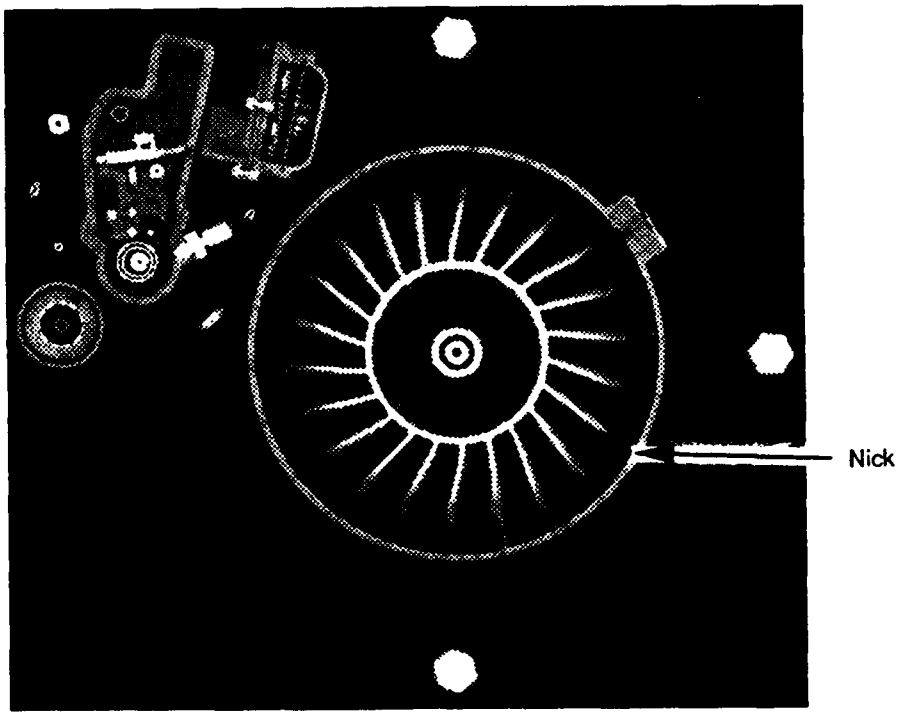

Figure 3.2-8 CT slice of the first axial compressor of the F107 engine on a 400 kV CT system (System L).

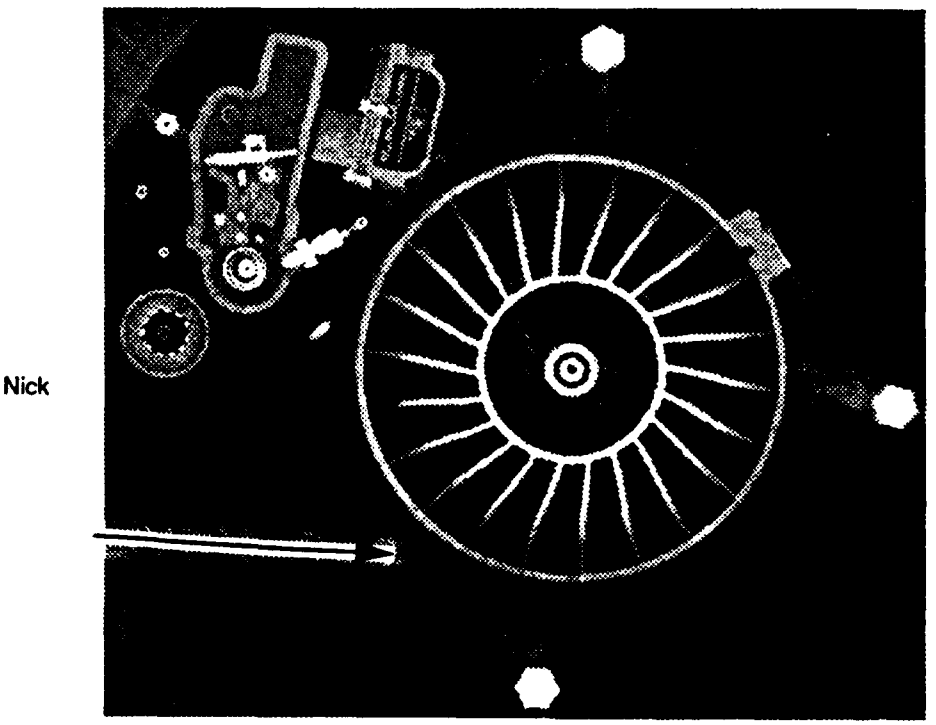

Figure 3.2-9 CT slice of the first axial compressor of the F107 engine on a 2.5 MV system (System S).

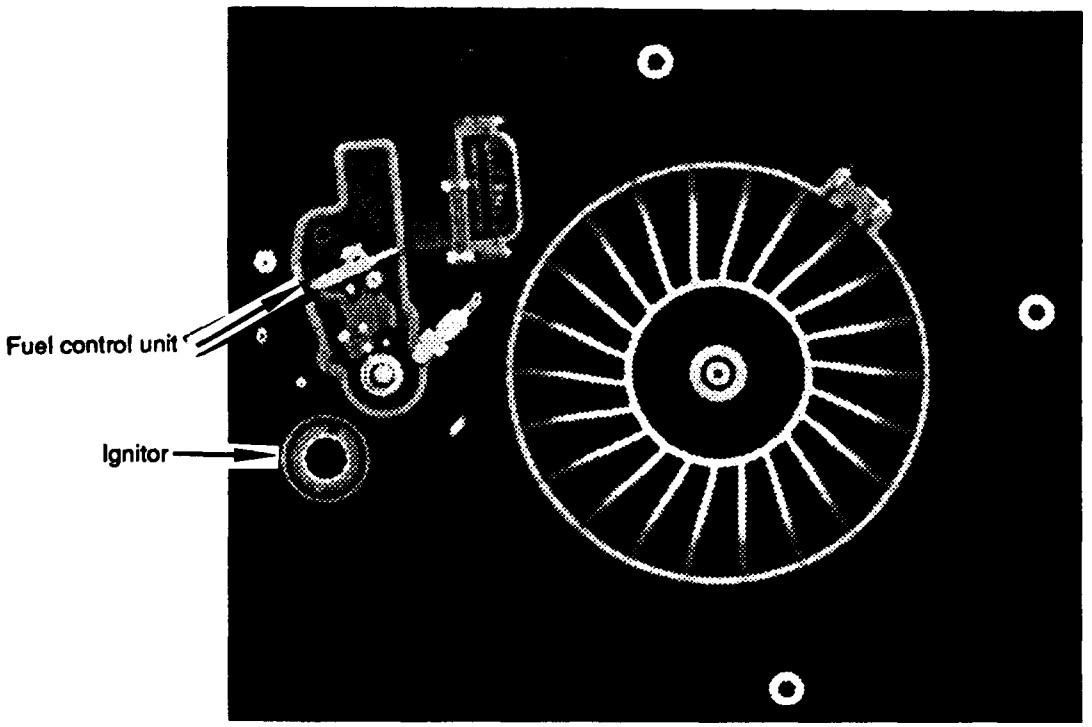

Figure 3.2-10 CT slice of the first axial compressor of the F107 engine on a 9 MV CT system (System U).

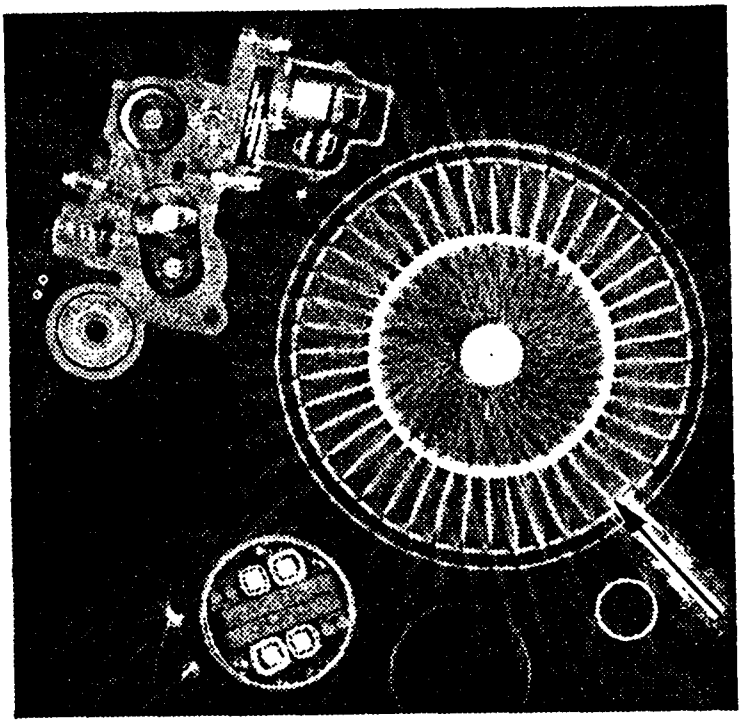

Figure 3.2-11 CT slice of the second axial compressor of the F107 engine on a 400 kV CT system (System L).

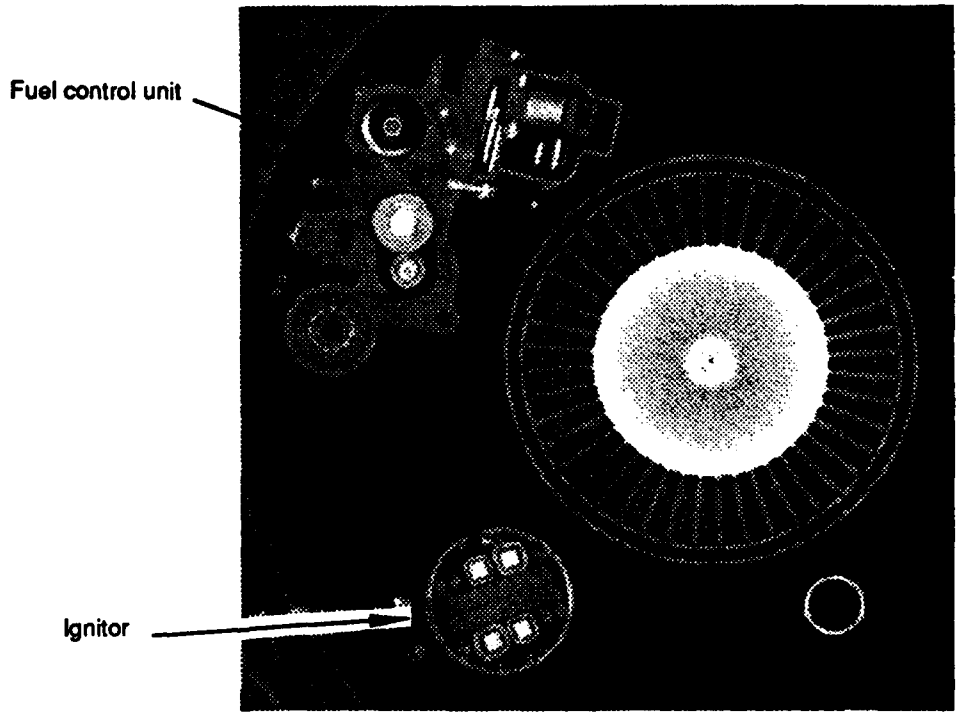

Figure 3.2-12 CT slice of the second axial compressor of the F107 engine on a 2.5 MV CT system (System S).

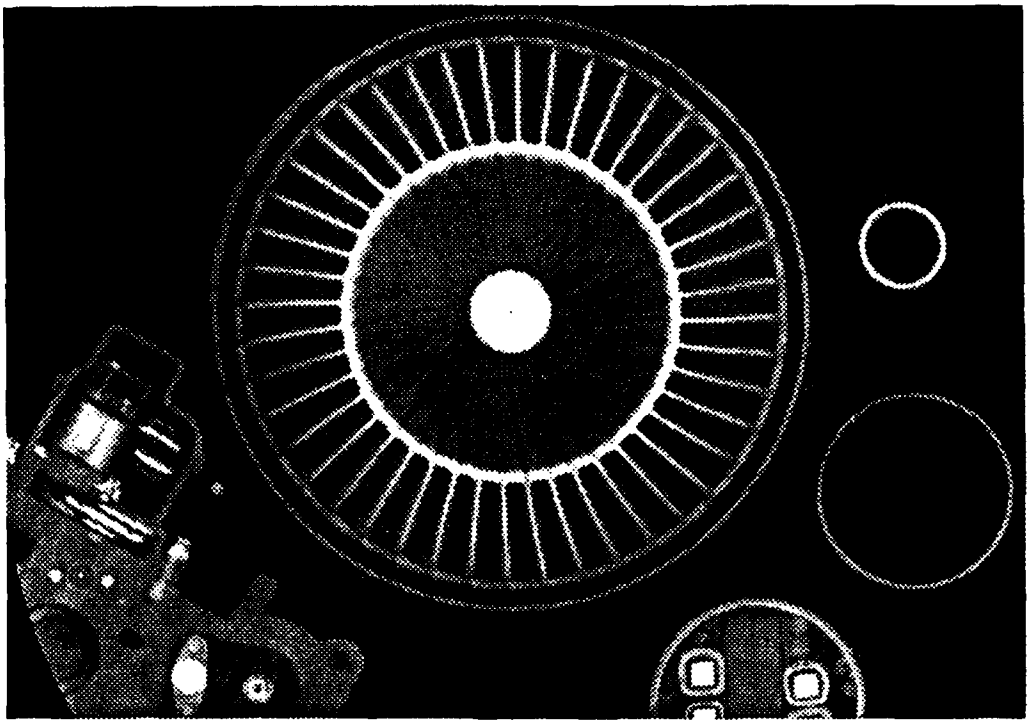

Figure 3.2-13 CT slice of the second axial compressor of the F107 engine on a 2 MV CT system (System H).

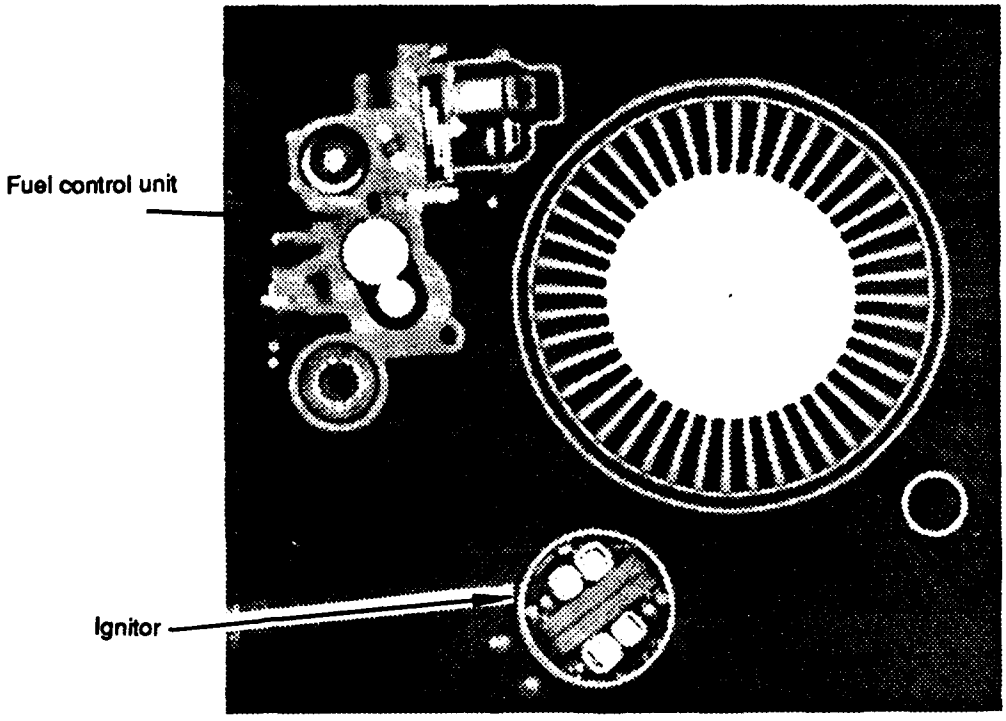

Figure 3.2-14 CT slice of the second axial compressor of the F107 engine on a 9 MV CT system (System U).

The second area of interest is the stator section of the engine, following the 4th compressor stage. Figures 3.2-15 through 3.2-17 are CT slices from 400 kV, 2.5 MV, and 9 MV systems, respectively, taken through the forward area of the stator section. The slices are not at identical axial locations. The effect of the X-ray system energy is apparent. The penetration of the higher energy system has reduced artifacts and shadowing from other features and thus provides better sensitivity to detail. The bearing detail around the main shaft is of interest. Figure 3.2-18 is a 9 MV image showing the gears in the gear reduction box. The detail in the gears indicate resolution on the order of 0.5 mm.

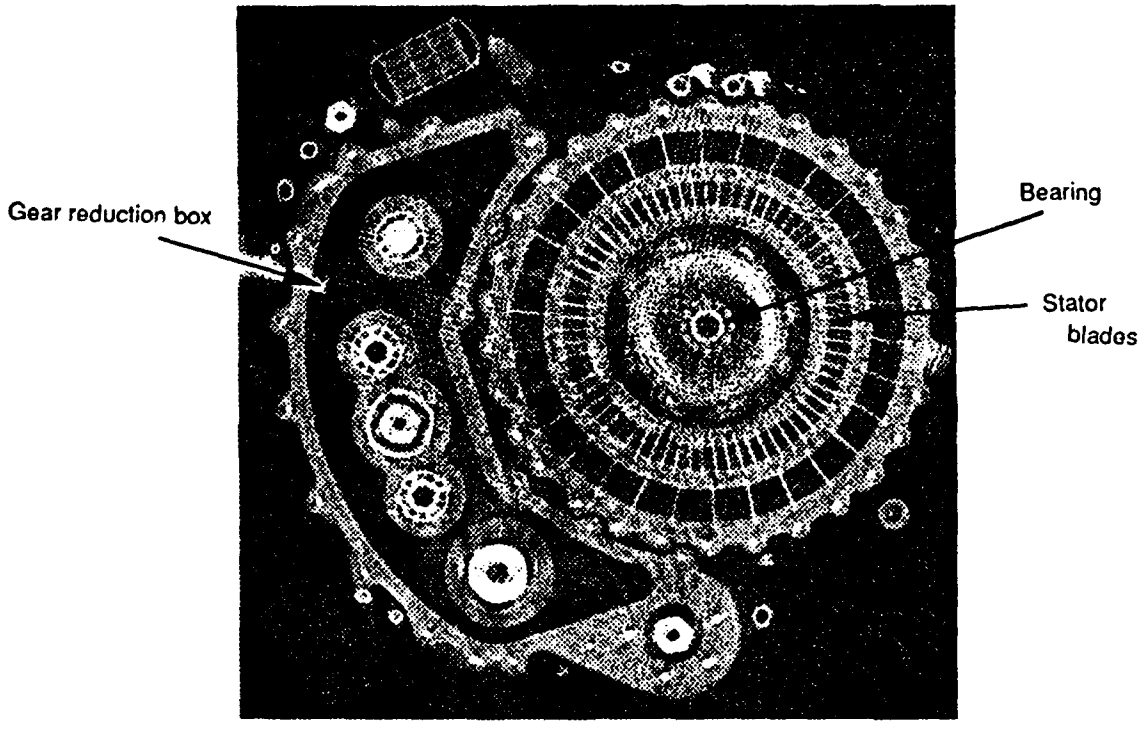

Figure 3.2-15 CT slice of the stator section of the F107 engine on a 400 kV CT system (System L).

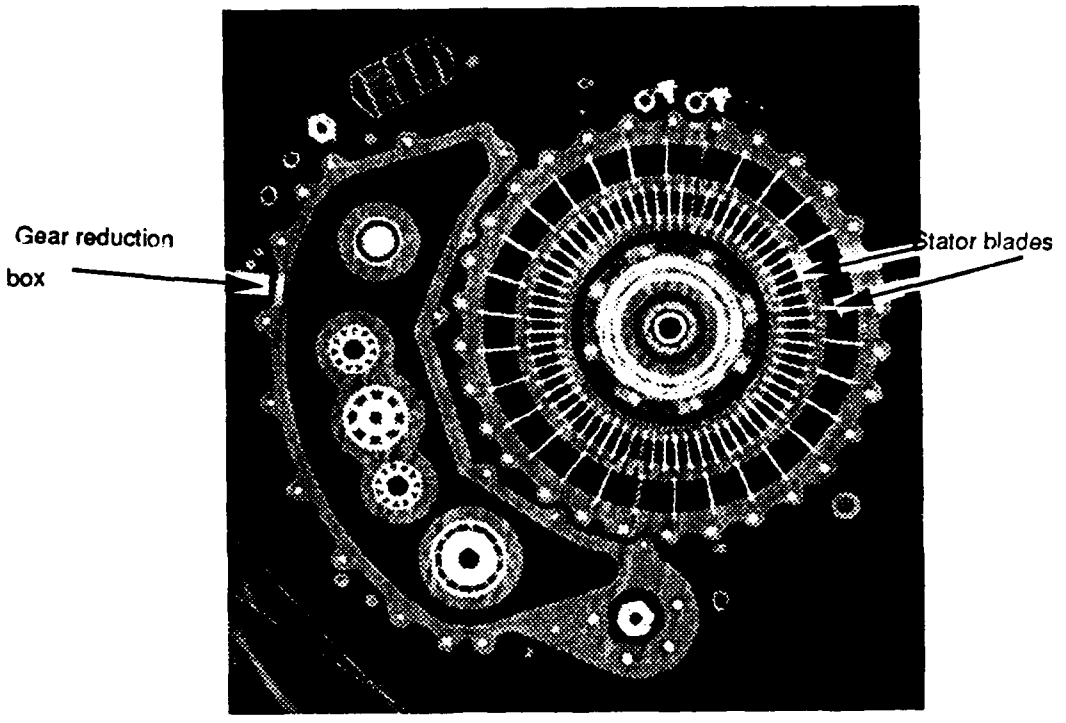

Figure 3.2-16 CT slice of the stator section of the F107 engine on a 2.5 MV CT system (System S).

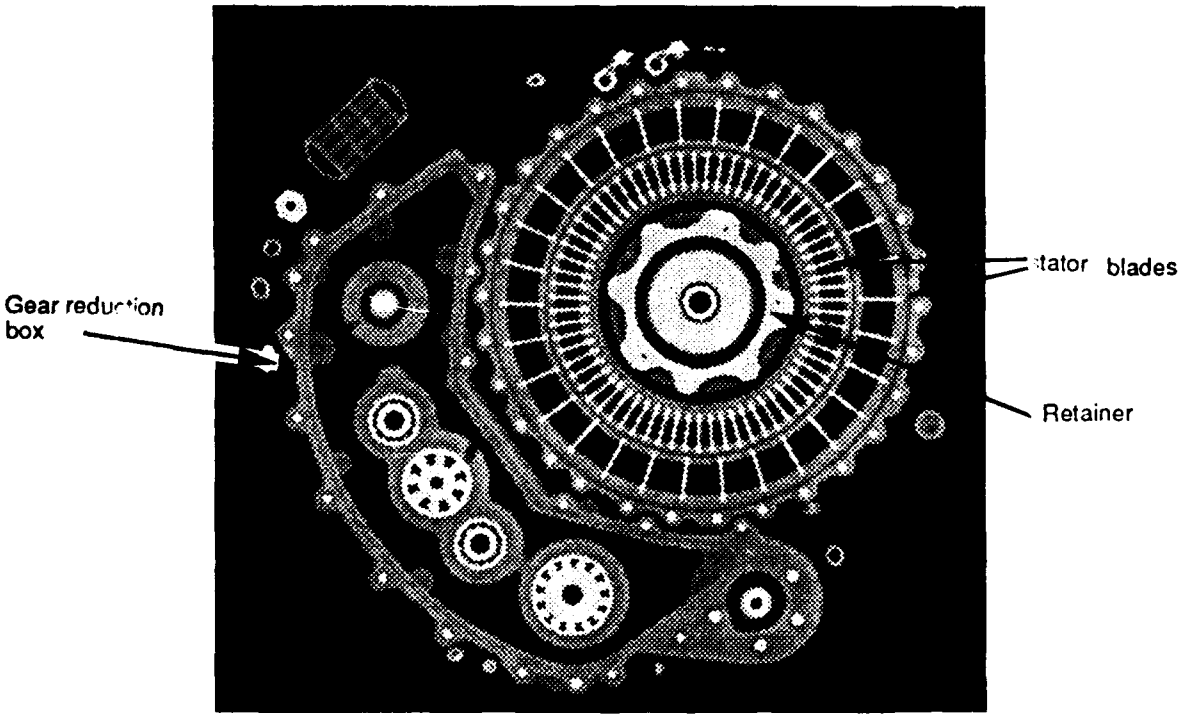

Figure 3.2-17 CT slice of the stator section of the F107 engine on a 9 MV CT system (System U).

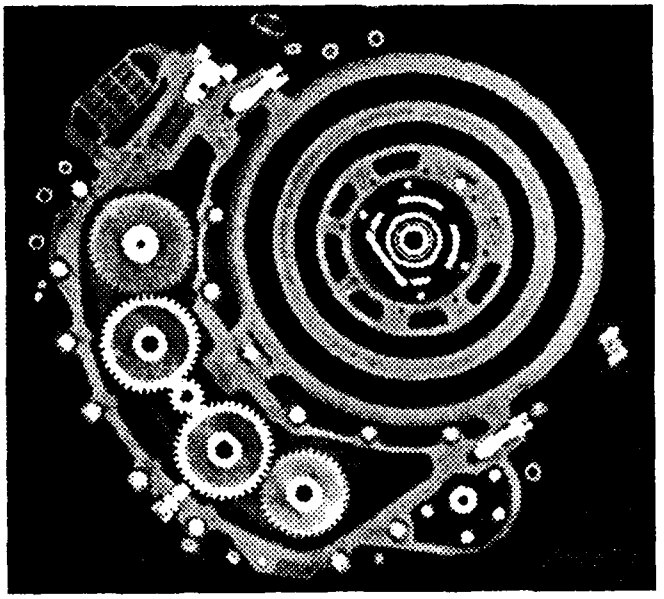

Figure 3.2-18 CT slice of the gears in the gear reduction box of the F107 engine on a 9 MV CT system (System U).

The third area of interest is the burner/combustor area. Figure 3.2-19 is a 9 MV CT slice taken in this region as noted on the longitudinal image, Figure 3.2-7. In the original image the air injection holes can be clearly observed, although reproduction reduces the visibility.

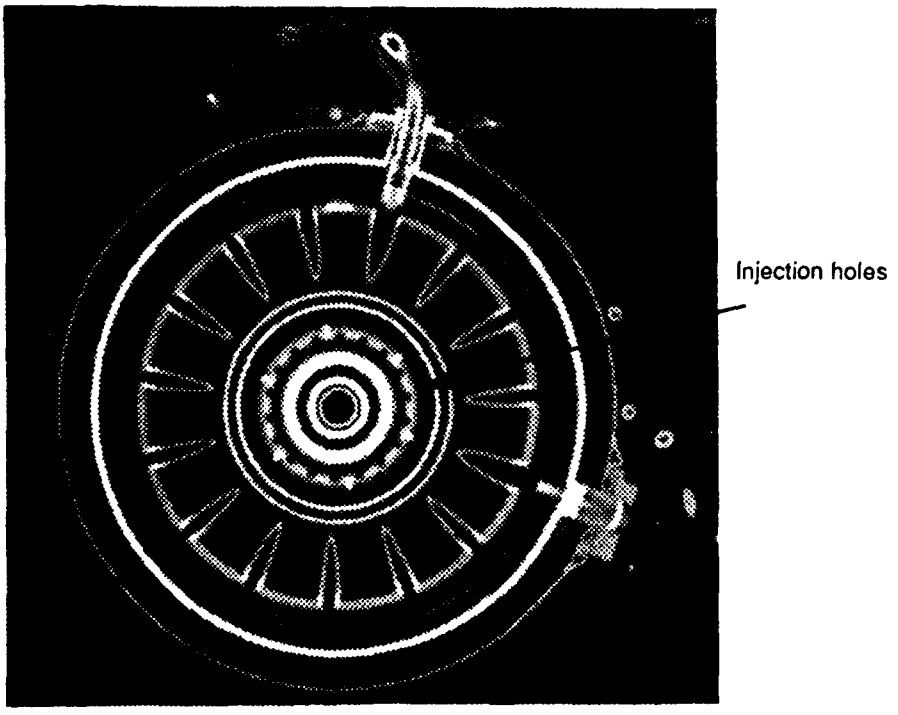

Figure 3.2-19 CT slice of the burner/combustor region of the F107 engine on a 9 MV CT system (System U).

The fourth area of interest is the labyrinth seal area following the burner/combustor area. This seal prevents hot combustion gases from exiting the combustor area along the drive shaft of the engine. Figure 3.2-20 is an enlargement of the labyrinth seal from the 2.5 MV longitudinal CT of Figure 3.2-5. Figure 3.2-21 is an enlargement of the labyrinth seal from the 2 MV system of Figure 3.2-6. Figure 3.2-22 is an enlargement of the labyrinth seal from the 9 MV system of Figure 3.2-7. Comparison of these images shows that the inherent resolution, reconstruction pixel size and signal to noise in the image are critical to observing detail in the engine. The 9 MV image, Figure 3.2-22, shows the best sensitivity in the main shaft of the engine as should be expected for the high energy. The 2 MV image of Figure 3.2-21 however appears to show greater detail in the labyrinth seal region. This 2 MV system image has good signal to noise and sufficiently defined pixels in the reconstruction field to show small fingers in the seal. All three images appear to show an inherent resolution of around 0.5 mm, however finer details are detected as the signal to noise increases in the image.

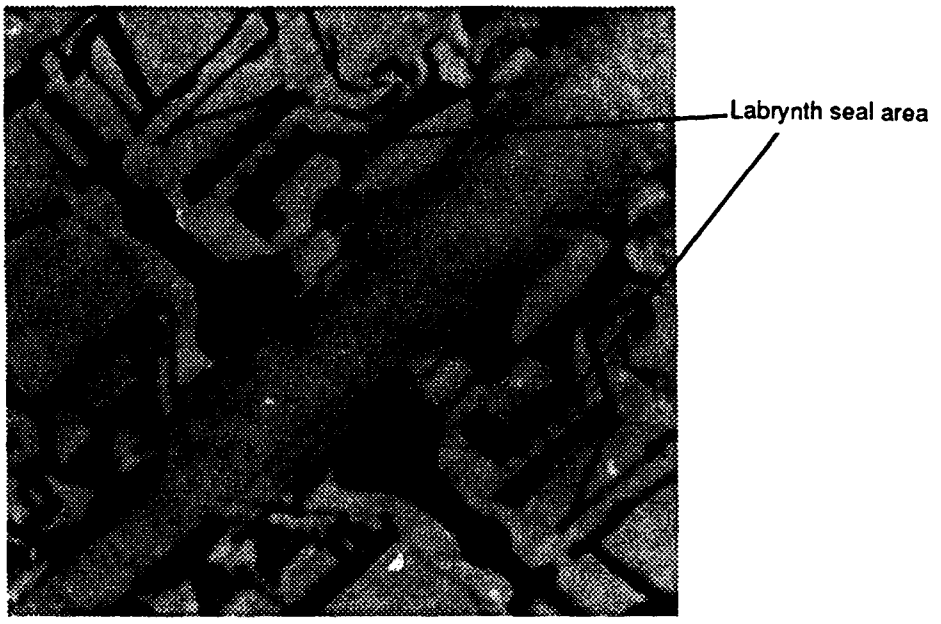

Figure 3.2-20 Enlargement of the longitudinal CT slice of the F107 engine from the Figure 3.2-5, 2.5 MV image to show the labyrinth seal (System S).

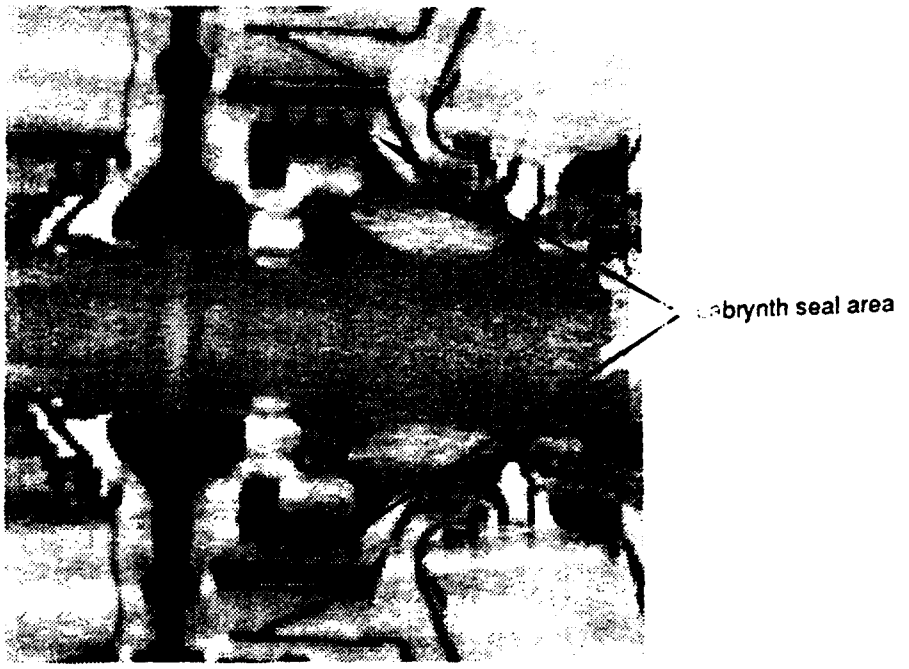

Figure 3.2-21 Enlargement of the longitudinal CT slice of the F107 engine from the Figure 3.2-6, 2 MV image to show the labyrinth seal (System H).

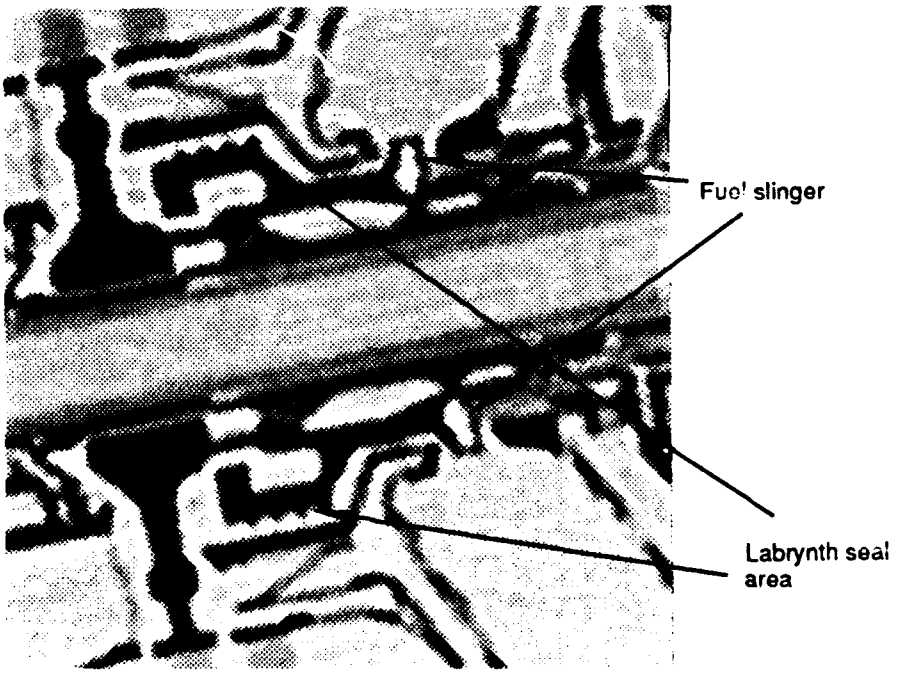

Figure 3.2-22 Enlargement of the longitudinal CT slice of the F107 engine from the Figure 3.2-7, 9 MV image to show the labyrinth seal (System U).

The fifth area of interest is turbine region. Figures 3.2-23 through 3.2-25 show CT slices from the 2.5 MV, 2 MV and 9 MV systems respectively. Figure 3.2-24 clearly shows a region of possible erosion on the side of the turbine casing. This detail was detected to some degree in the other images but the slice positions are slightly different on the turbine. These images were not taken through the center of tubine disk. The turbine disk is a high temperature alloy which creates significant attenuation for the 2 MV CT systems. The 9 MV energy would be adequate for this size and material of turbine.

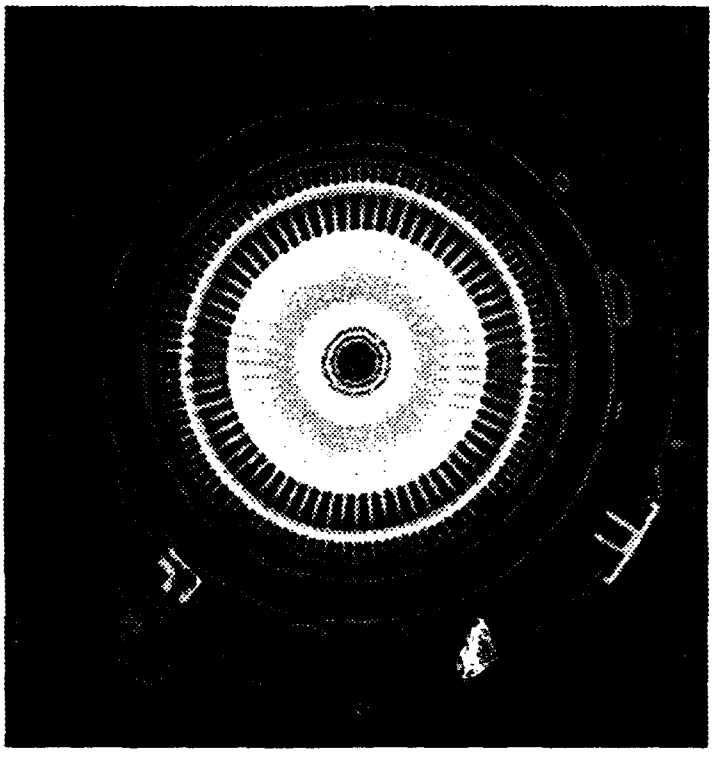

Figure 3.2-23 CT slice of the turbine of the F107 engine from a 2.5 MV CT system (System S).

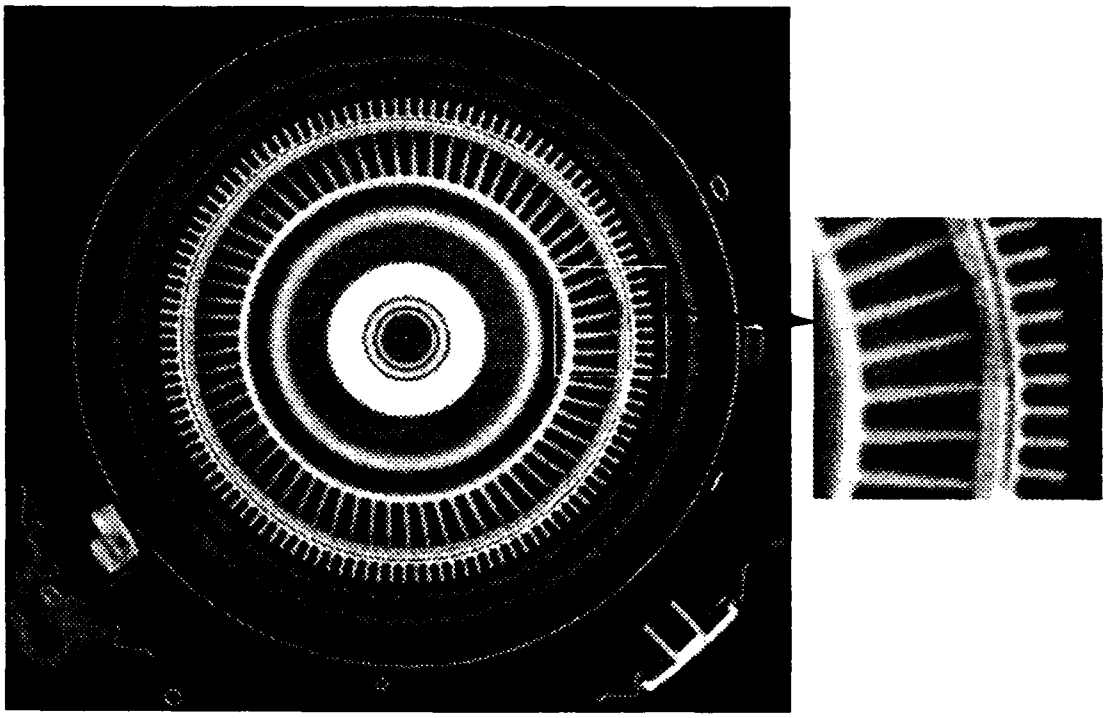

Figure 3.2-24 CT slice of the turbine of the F107 engine from a 2 MV CT system (System H) and enlargement of eroded region.

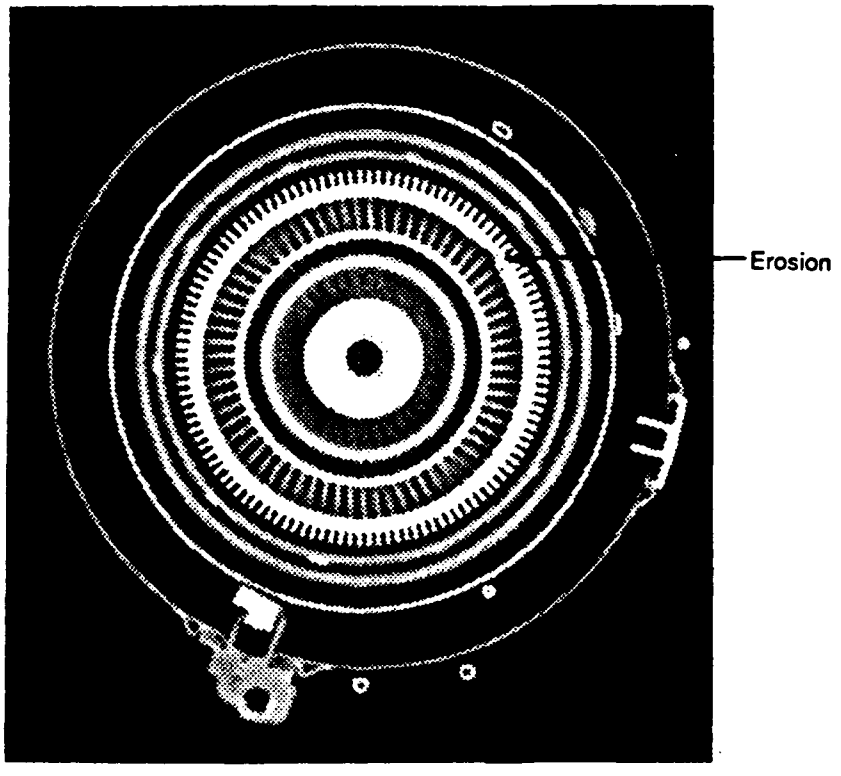

Figure 3.2-25 CT slice of the turbine of the F107 engine from a 9 MV CT system (System U).

3.2.2 Teledyne Helicopter Drone Engine

The Teledyne J402 engine is an air impingement or windmill start turbojet, with a single entry, ram air inlet featuring two transonic axial compressors plus a centrifugal compressor, an annular combustor and a single stage axial flow turbine. It produces a maximum of 980 pounds of thrust at 41,500 RPM. The engine is 85 cm (33.3 inches) long, 32 cm (12.5 inches) wide and weighs 63 kg (138 pounds). Figure 3.2-26 is a photograph showing the Teledyne engine.

The Teledyne engine was scanned only on the 400 kV and 9 MV CT systems. Due to system availability constraints no longitudinal scans were taken on the 9 MV system and the 400 kV CT system did not have sufficient energy for a longitudinal scan. Image details generally are the same as those of the F107-WR-400 CME for regions such as the compressor, stator and turbine. Figure 3.2-27 is a CT slice taken with the 400 kV CT system through the fuel slinger region of the burner can. This region was of particular interest to check for blockage in the fuel holes, which appear to be clear. A 400 kV system is capable of imaging details in this region of an engine with adequate sensitivity to image the fuel holes, checking for blockage.

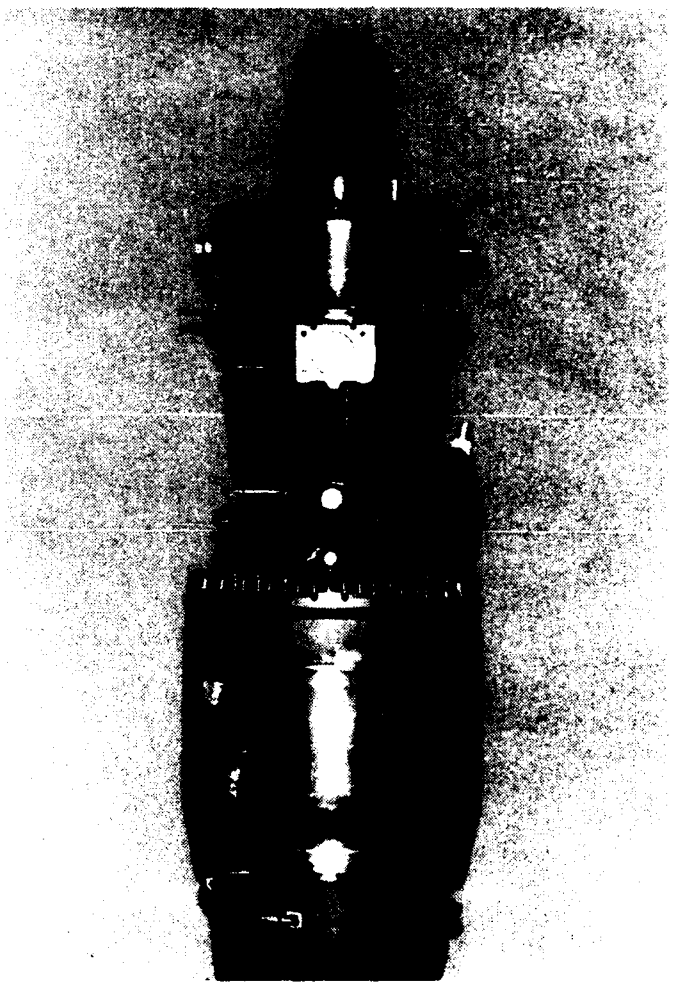

Figure 3.2-26 Photograph of the Teledyne J402 engine.

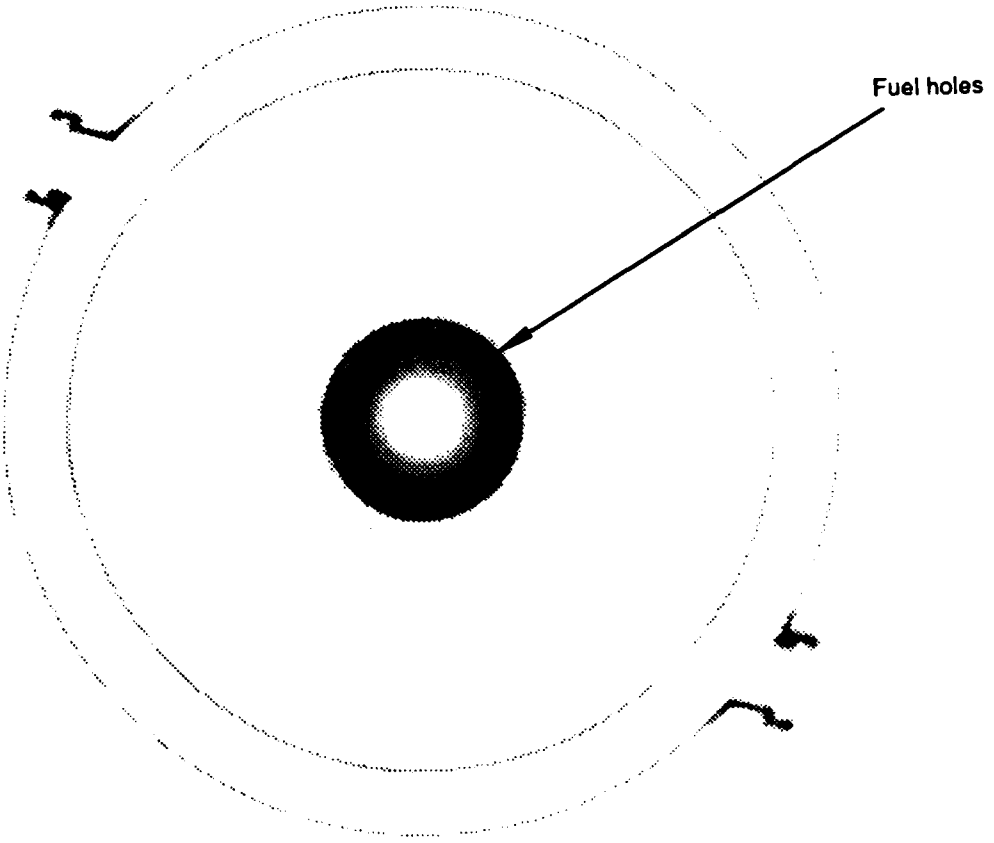

Figure 3.2-27 CT slice of the fuel slinger of the Teledyne J402 engine from a 400 kV CT system (System L).

3.2.3 Damaged ALCM Engine

The F107-WR-101 CME used in the Air Launched Cruise Missile (ALCM) is a non-augmented, twin spool, axial flow turbofan engine with a mixed exhaust. The low pressure spool consists of a two stage axial fan followed by two additional axial compressor stages in the gas generator flow path, these are all driven by two axial turbines. The high pressure spool consists of a single stage centrifugal compressor driven by a single axial turbine. The shafts are counter-rotating to minimize gyroscope and shaft vibration effects. The engines use a folded annular burner with rotary fuel injection. It provides a maximum of 600 pounds of thrust and is approximately 109 cm (43 inches) long, 36 cm (14 inches) wide, 53 cm (21 inches) high and weighs 71 kg (156.5) pounds.

An F107 ALCM engine which had crashed and burned was obtained for CT scanning. The purpose was to attempt to identify internal features. Figure 3.2-28 is a photograph showing the burned engine. The burned ALCM engine was scanned only on the 400 kV CT system. A CT slice, shown in Figure 3.2-29, through a compressor stage shows the distortion and damage that resulted from the crash and fire. The external and internal damage was so severe as to be obvious, but CT did show that molten metal that had solidified internally. The use of CT to image the damaged interior could provide information about fire temperature (dependent on metals that melted) and position (where metal pools solidified). This however was not pursued in this case.

Figure 3.2-28 Photograph of the burned ALCM engine.

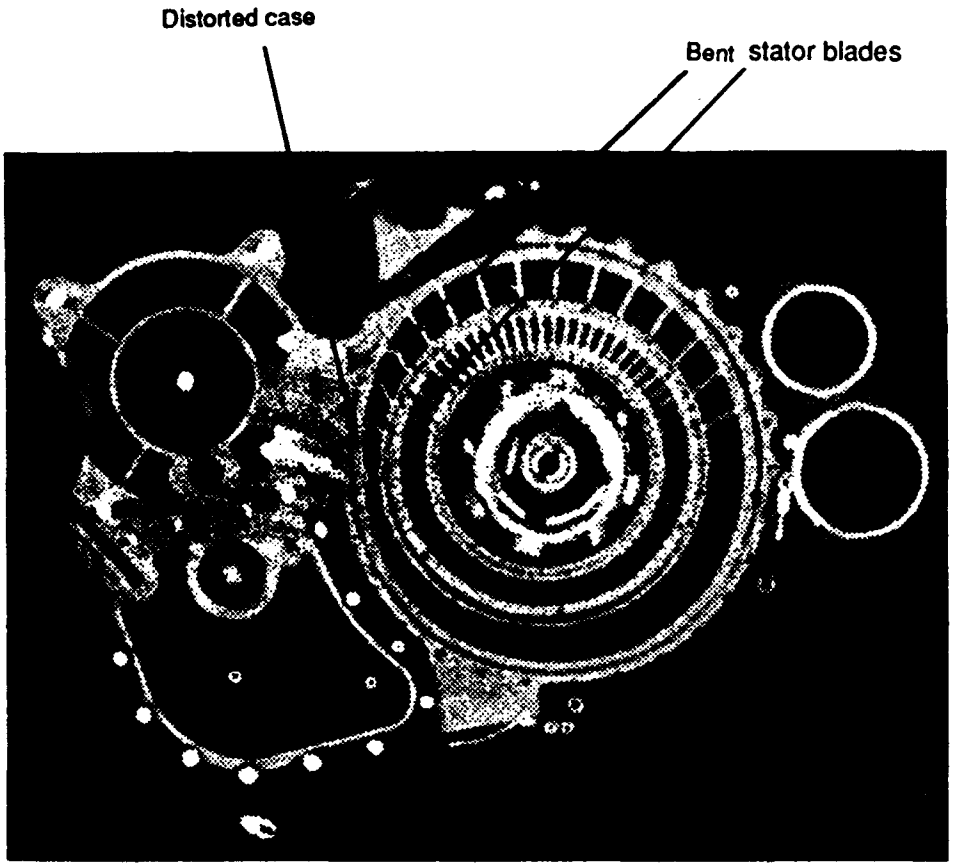

Figure 3.2-29 CT slice of the compressor stage of the burned ALCM engine from a 400 kV CT system (System L).

4.0 CENTER OF GRAVITY MEASUREMENT

Vibration must be kept to a minimum in jet engine assemblies, requiring extensive testing of subcomponents and the full assembly, with disassembly and rebalancing operations being iteratively performed until the individual components of the system are in proper tolerance. For example, the Air Force repeats the cycle of dynamic balancing and grinding on nominal small jet engine parts until the measurement is accurate to about 0.28 g at 3 cm (0.9 g-cm). CT cross section data contains measurements of the material and position such that the prediction of the CG of an object is theoretically possible.

The practical accuracy of the prediction, based on CT data, will depend on a number of parameters such as the CT system resolution, contrast sensitivity, mechanical accuracy, the complexity and density variation in an object, influence of adjacent features on the measurement of the feature of interest and partial voluming of features in the CT slice. A first question in the evaluation of using CT for component CG measurement is the level of accuracy possible on a simple geometry test phantom. If the simple test phantom CG measurement accuracy is sufficient, then complexity and adjacency of structure in an actual engine will require additional evaluations, not covered in the preliminary study of this task, to determine the ultimate applicability of CT for CG on whole systems.

4.1 CT Approach

The CG for a 2 dimensional object can be broken out into x and y CG positions relative to a part fixed coordinate system and represented mathematically as

$$X_{CG} = \sum\sum \rho_{ij} * x_i \,/\, \sum\sum \rho_{ij} \qquad (1)$$

$$Y_{CG} = \sum\sum \rho_{ij} * y_j \,/\, \sum\sum \rho_{ij} \qquad (2)$$

where ρ_{ij} is the density value at the ij position, x_i is the x dimension distance to the ith position and y_j is the y dimension distance to the jth position. In order to test the ability of CT slices to provide measures of the CG a test phantom, described in Section 2.1, has been imaged at a height to form two concentric rings in the image, one of which may be a bushing that has missing (removed) material. The CT data from the phantom is appropriately processed to measure the CG.

Four computer routines (CIRNOT, COGP, RRADII and CENTROID), operating under the INDERS data analysis package [9], have been used to calculate the CG. The routines extract information from the images of the test phantom, but use two different approaches for the CG calculation. One approach, using CIRNOT and COGP, calculates the CG assuming a uniform mass for the material in the phantom. The second approach, using RADII and CENTROID, use the CT density values across the phantom image in the calculation of CG. The test phantom CG measurements are measured as shifts from the physical center of the outer ring.

The CIRNOT routine processes the phantom image to form contours using a 50 percent threshold. For the test phantom images, four contours are created. The COGP routine assumes that contours alternate between uniform material and air. The COGP routine then processes each contour to calculate the "center of area" of the pixels inside each contour. Thus the outermost contour would create the center of area for an entire disk. However when COGP processes the second contour, it subtracts this area, leaving the center of area of the outer ring. When the third and fourth contours are processed, the center of areas for the bushing is added to the center of area for the outer ring. If the material is uniform, the center of area is equivalent to the CG. The

relative CG position for a change in the test phantom is measured by taking the difference between the CG of the entire phantom (where the bushing has been moved or changed) and a reference center of the part which is assumed to be the CG of the outer ring (which does not change).

In the second approach, the RRADII routine searches from the edge of the data set until it finds the threshold density value then performs a bilinear interpolation on the previous pixels data to find the edge more precisely. It performs this process for 24 different angular orientations and then iteratively calculates the center of each radius from the detected edges. This calculation provides a reference geometric center of the part in the CT image coordinate system, assuming that it is adequately represented by the outside diameter of the test phantom. The CENTROID routine processes the CT image to calculated CG using the "CT density" values present in the image using equations (1) and (2) above. A 50 percent threshold edge detection algorithm is applied to determine the edge of material and air. The calculated CG is compared to the reference geometric center of the part obtained from RRADII.

For a material of high density variation, the second approach would be expected to be more accurate. For homogeneous materials, the first approach, area calculation, has advantages in speed and possibly accuracy because the edge effect and beam hardening density variations do not influence the calculation.

4.2 CT Measurements

CT scanning of the test phantom was performed so that the CT slice imaged the outer ring and inner bushing. The CT slices were taken of the test phantom in five different configurations as designated in Table 4.2-1 and using both 180° and 360° scans. The three inner bushings had 0, -0.5 and -1.0 g of material removed as a flat on the outer edge of the bushings. The scanning of the phantom was performed with the flat oriented in the 0° or 180° position, so that a shift of the CG would occur between scans of each trimmed bushing. Two scans were taken at each configuration to test for consistency in the data.

Table 4.2-1 Phantom Scanning Conditions

Condition	Flat Type	Flat Weight	Orientation
1	None	0.0 g	0°
2	Small	-0.5 g	0°
3	Small	-0.5 g	180°
4	Large	-1.0 g	0°
5	Large	-1.0 g	180°

Figure 4.2-1 is an example CT slice of the test phantom. In this image the bushing has 0.5 g removed in the 0° orientation.

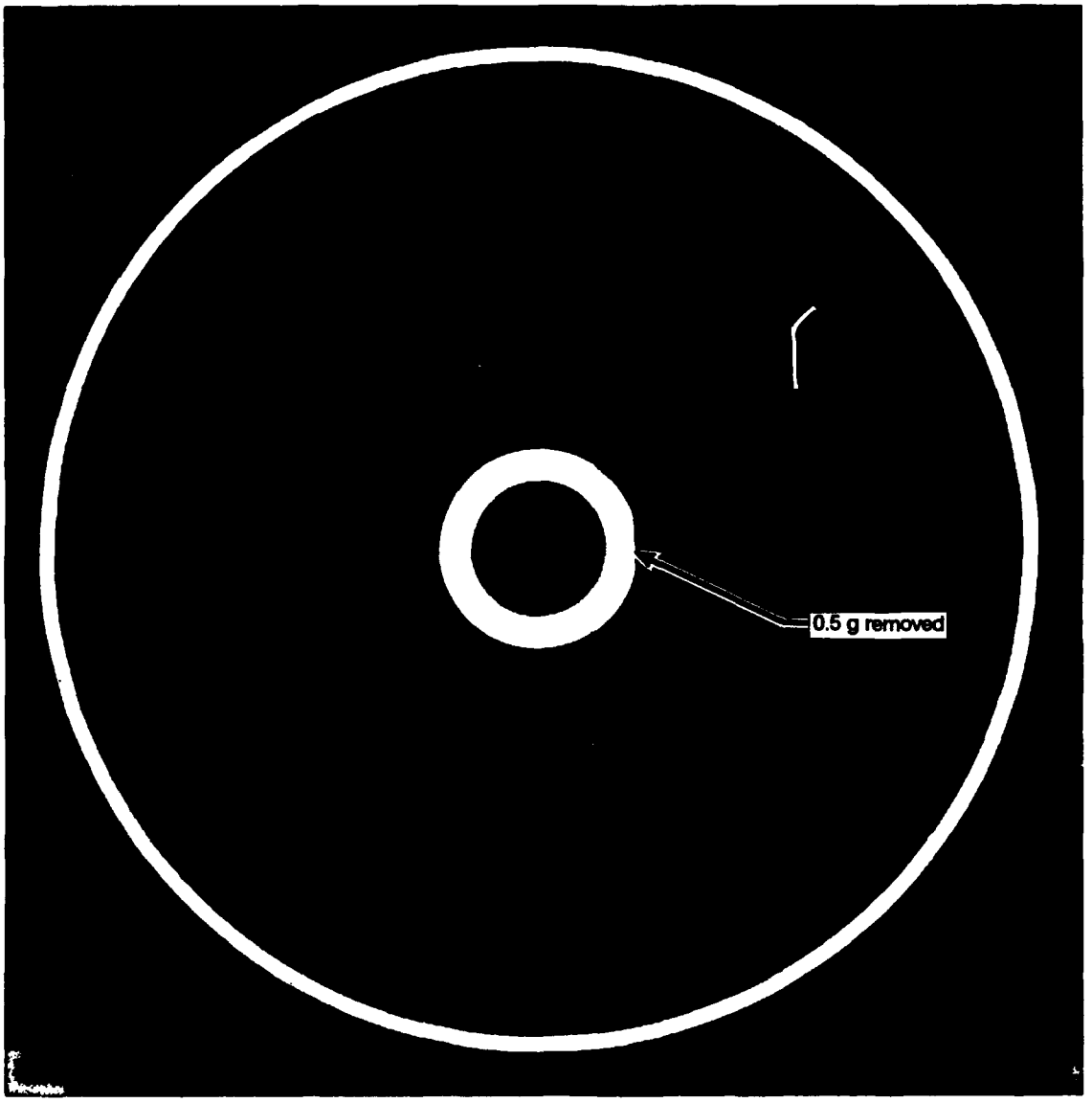

Figure 4.2-1 CT image of the CG test phantom with 0.5 g removed.

The CG calculation is dependent on thresholding of the image data. A sensitivity study for threshold value found that as long as the same threshold value is used, for all scans of the same material, the CG calculations are relatively unaffected by the value selected. The value selected was 50 percent of material density. Because of the design of the phantom, the CG measurements were plotted in terms of the shift in the CG as the bushings were changed and rotated. The shift is compared to the outer ring of the phantom center as discussed in Section 4.1. The outer ring remains fixed in this experiment and the change in the bushing is monitored as a measure of the ability of CT to monitor CG.

Figure 4.2-2 and 4.2-3 show plots of the difference between the outer ring center (R_x) and the CG (C_x) as a function of mass shift. Because the inner bushing has been rotated 180° between scans, the measurements show the effect of x axis CG. The change in CG from the 0° to the 180° rotation on the y axis is zero. Figure 4.2-2 is for the case of 180° scanning on the CT system and Figure 4.2-3 is for 360° scanning. In each image the plots are for the "center of area" and actual "CT density" value approaches. Both figures show that the slope of the mass shift is the same for either approach. The multiple scan results, lie on top of one another except for the 180° "CT density" case. The figures show that there is an offset in the CG position between the two approaches and that CG at 0 g mass shift is not necessarily the center of the test phantom. This result indicates that how the images are processed can introduce an offset in absolute CG calculation. The figures indicate the sensitivity of CT to changes in the CG of a system of better than 0.25 g in the test phantom. This is shown as a measurement of the CG shift on the order of 0.03 mm, which is less than one-tenth of the pixel size in the image.

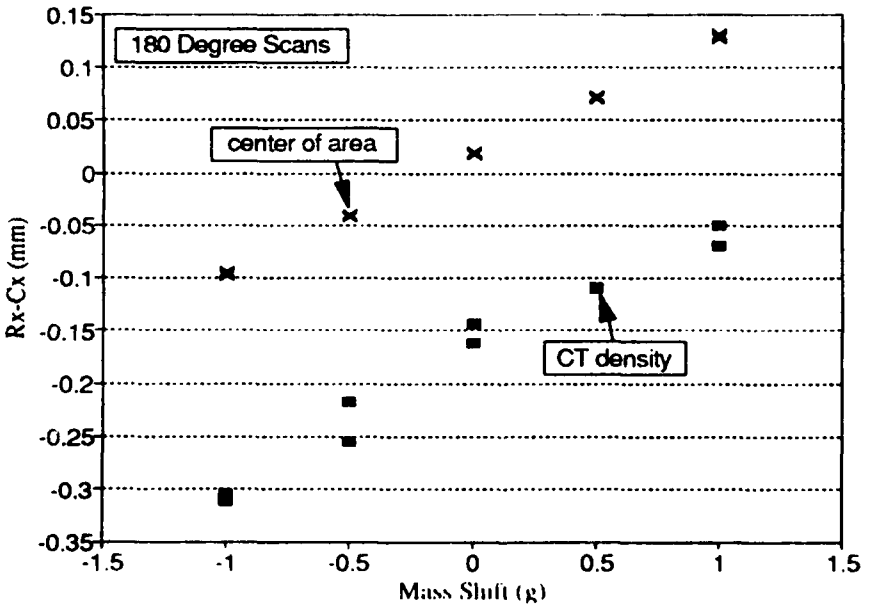

Figure 4.2-2 Difference between center of geometry and CG for 180°o scans.

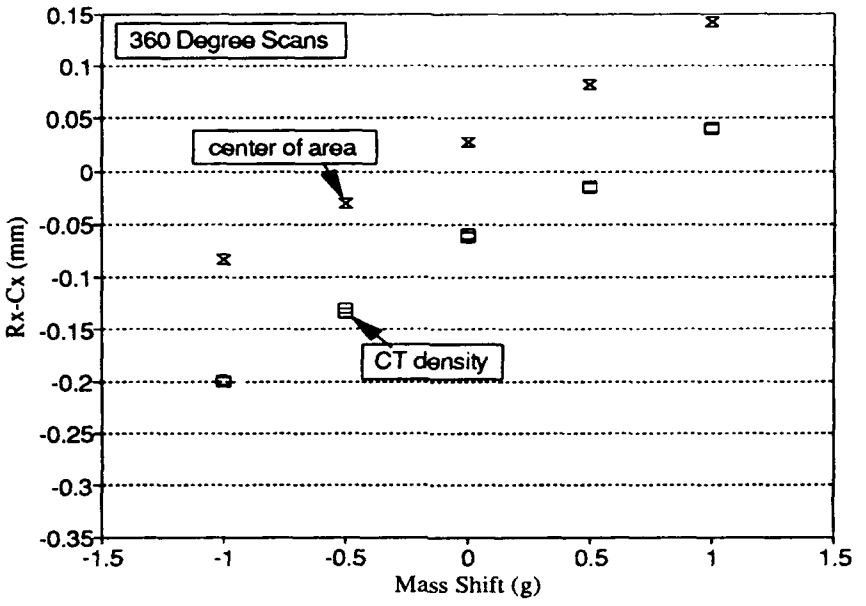

Figure 4.2-3 Difference between center of geometry and CG for 360°° scans.

Figure 4.2-4 shows a plot of the CT CG measurement shift versus the mass shift. The figure contains plots for the theoretical shift that would be expected, and for the 180° and 360° scanning using both "center of area" and actual "CT density" values. These curves show that the CT measurements fall within 0.05 mm (1.6×10^{-4} of the dimension of the scanned part) of the theoretical prediction. The rotation of the bushings between + and - mass shift was not precisely indexed which may account in part for the deviation from the theoretical curve for the + to - mass shift.

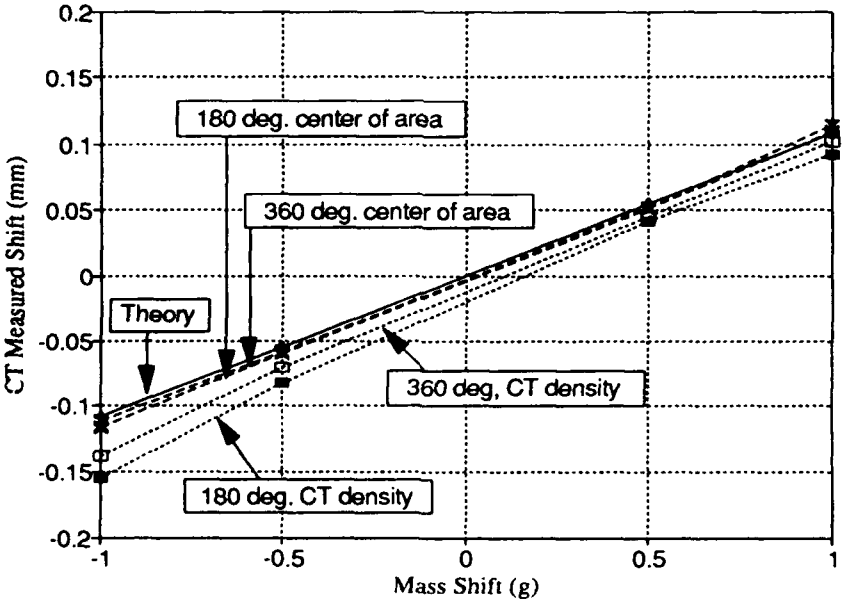

Figure 4.2-4 Comparison of the shift in the CG for a mass shift in the test phantom including the theoretical shift.

4.3 CG Discussion

The results of the CG study indicate that CT measurements are very sensitive to changes in the CG of objects. The absolute position of the CG however varies depending on the calculation technique. The "center of area" measurement approach for data processing appears to be fairly accurate with measurements within 0.025 mm (0.001 inch) for the uniform phantom. The actual "CT density" approach is less accurate than the "center of area" approach, with the CG being misplaced by up to 0.05 mm (0.002 inch) for 360° tomographic scans and 0.15 mm (0.006 inch) for 180° scans. This offset for the "CT density" approach is believed to be due to the CT system effects that are consistent and therefore it should be possible to establish factors to correct for it.

The volume of the CT slice taken through the body of the part is proportional to the CT slice thickness. Testing of the CT system used in the CG scans with a slice thickness phantom has shown that the beam is of approximately uniform thickness over the scan plane for the CG test phantom. An effective slice thickness of 2 mm was used for the CT scanning. Thus the CT measurements on the 10 mm thick bushings (for which 0.5 and 1.0 g of material had been removed) were actually indicating a sensitivity to two-tenths of the bushing material (or 0.1 and 0.2 g respectively) of the material removed. Thus the ability to measure to an approximately 0.25 g mass shift accuracy from Figures 4.2-1 and 4.2-2 curves at the 3 cm bushing radius is actually a sensitivity to about 0.15 g-cm.

The area change due to the change of 0.5 g in the aluminum bushing is approximately 225 parts in 60,000. For a higher density object than aluminum, a mass shift of 0.5 g will be proportionally smaller by the ratio of the densities. The percent error in the area measurement will increase proportionally also. The CT data analysis shows that the CT image area variation from multiple scans of the phantom is approximately 3 parts in 60,000, which is negligible for the whole assembly and 3 parts in 225 (1.3 percent) of the 0.5 g aluminum bushing area.

CT scanning of the CG test phantom on additional CT systems showed generally the same results as those presented. In one case however a lead marker was introduced into the field of view on a 9 MV CT scan. This adjacent structure affected the result significantly enough that the calculation could not be made using the software developed in this study. This indicates serious concerns about applying the CG measurement when surrounding structure in the CT slice is static. The approach that may be applied in this situation, is to measure the CG at two positions of the rotational hardware while the static, adjacent hardware remains fixed. Any shift in the CG will be due to imbalance in the rotating hardware. It is expected that the accuracy of this approach will be affected by the relative magnitude of the material that is static to the material that is rotating.

Overall this preliminary study of CT measurement for CG indicates that additional work will be needed to develop the capability for whole systems. The affect of outside structure and of material in the CT slice that is varying in shape across the CT slice plane will need to be examined. There appears to be good reason to believe that differential measurements of the CG for two positions should be a good approach. The design of a new, more complex test phantom, that will allow dynamic balancing to compare with CT measurements is the next logical step. Attempts to experimentally determine the center of mass by the two scale method on the existing phantom would have only been sensitive to 0.1 g (±0.1 g) at 30 cm, where the measurements of 0.1 g at 3 cm (0.01 g at 30 cm) in the -0.5 g case were needed.

5.0 COST BENEFIT ANALYSIS

A CT evaluation system has the capability to have an impact on cost, confidence and time required to maintain and repair whole systems. Several of the benefits of CT inspection are: inspection without disassembly, dimensional measurement, foreign object or debris detection, density determination, corrosion or corrosion effects detection, geometry acquisition for CAD/CAM and possibly for center of gravity calculation on components or rotating subassemblies.

Particular benefits can be derived for systems where disassembly for internal inspection is cost and time prohibitive. Specific examples would be single use weapon systems such as cruise missiles, some of which are assembled from castings and have large portions of their primary structure which can not be inspected after assembly. These types of systems come into the depot at regular intervals for Analytical Condition Inspection (ACI) and the restraints of their construction, budgets, time and personnel place limits on this investigation.

An example of the savings that could be realized utilizing CT would be in the area of cruise missile engine inspection. Being a single use system a majority of the engines are returned to the depot without having been run since the last depot or manufacturer maintenance. It should be feasible to perform CT evaluation and power test, eliminating the disassembly (and all that it entails) until such time as the bearings and seals or soft parts would require replacement. The existing data base on engine maintenance and reliability should have adequate information to allow tailoring of the maintenance cycle to accommodate the changes in inspection procedures and cycle time to allow the use of CT evaluations. This change would eliminate many of the operations currently performed including the disassembly which results in the need to rebalance rotating components and assemblies. Only in the instance of failing a power test vibration characterization, or another inspection would it be necessary to disassemble the engine at the minor overhaul interval. The feasibility of this approach is based on information on the operations currently performed at both major and minor intervals and the fact that a significant portion of the operations performed are clean and inspect nondestructively at the component level.

The CT evaluation approach could alter the evaluation plan for engines by monitoring assembly integrity, including component location, fuel and oil line orifices and rotating component clearances, in the maintenance cycle. This would eliminate or reduce overhaul steps such as disassembly, removal of accessories, physical cleaning, visual inspection, measuring, balancing, and reassembly of the cruise missile engine. This portion of an overhaul is estimated to take 55-65 labor hours and 1 week of flow time [10]. The savings in changing this process to CT evaluation can be significant depending on the number of engines maintained. For example, by 1995 the Air Force Oklahoma City ALC expects to service 500 engines/year. Assuming that CT could provide a 60 hour labor savings on average (the CT labor is included in the CT operating expense) for CME inspection, then Figure 5.0-1 shows the cost savings that would result if CT were employed. The calculations assume a $2.5M CT installation with an operating expense of $375K/yr. Figure 5.0-2 shows time to return the investment in the CT facility as a function of the number of engines maintained per year. At the 500 engines/yr level of effort, payback would occur in just over two years. The validity of this estimate is dependent on the ability to substitute the detail sensitivity of CT for the sensitivity of disassembly.

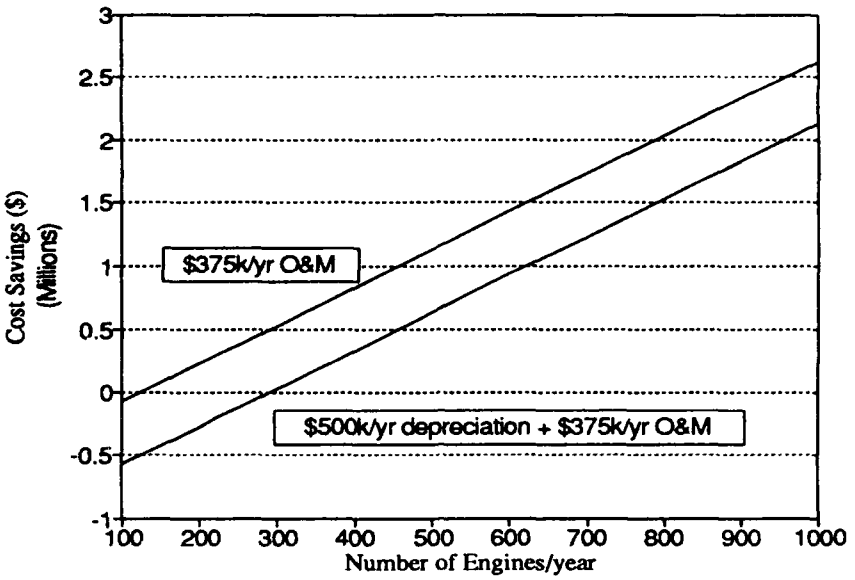

Figure 5.0-1 Cost savings as a function the of number or engines evaluated with CT.

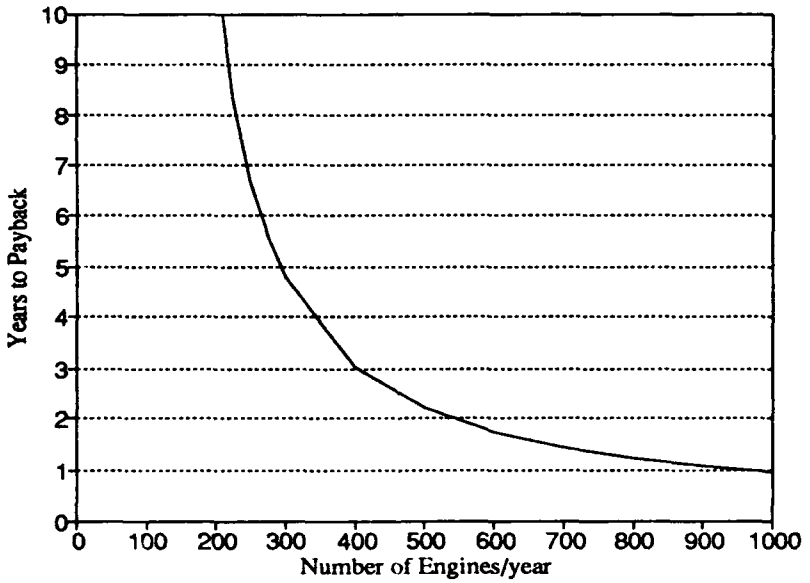

Figure 5.0-2 Years to payback a $2.5M CT system with an operating budget of $375K/yr as a function of the number of engines evaluated with CT.

Many of the auxiliary pieces that are used with the jet engines would also be candidates for CT inspection such as actuators, gearboxes, fuel controllers, inlets and nozzles. In the case of an Air Launched Missile Analysis Group (ALMAG) CT would allow the collection of physical information at the whole or assembled system level before the act of disassembly changes or obliterates it.

6.0 CONCLUSIONS AND RECOMMENDATIONS

6.1 Conclusions

Computed tomography provides cross sectional image information useful for the evaluation of whole systems, such as engines, for assembly verification and foreign object detection. CT, as part of an engine maintenance program, could assist by reducing the disassembly activity with a potential for reasonable economic return on investment. The ability to be sensitive to internal details generally increases with the CT system energies used from 400 kV to 2 MV to 9 MV. For long metal paths the highest energy available is preferred, however many of the 2 MV images can show good sensitivity to internal details, and even 400 kV can be usefully employed in some regions of an engine.

Experiments from a test phantom show that it is technically feasible to use CT data for measurement of the CG. The method as demonstrated with a ring test phantom is sensitive to within 0.15 g-cm at 3 cm radius in aluminum. The absolute position measurement with CT may be subject to an offset that will require correction if a single CT measurement is used. The preferred technique is to use 360° scans and a comparison of the CG shift between multiple positions. The influence of adjacent structure has been shown to greatly affect the CG calculations. Compensating for static adjacent structure may be possible by performing the CT measurement of CG using multiple rotational positions. The presence of the static structure would be expected to reduce CG measurement accuracy in proportion to the relative mass that is present. It should be noted that this technique is not limited to circular or high degree of symmetry parts but is applicable to parts with complex geometry.

6.2 Recommendations

CT examination of engines should utilize as high an X-ray energy source as can be practically obtained. In addition, due to the complexity and detail of the parts examined under this task assignment, it is recommended that 360° tomographic scan and reconstruction, region of interest or larger format image matrix reconstruction, and a high signal to noise (>50:1) are highly advisable. The use of 360° tomographic scanning is essential for measurements such as CG, and advised for detail evaluation across a complex system. The reconstruction pixel size should be on the order of one-half the inherent resolution of the CT system. Thus as the system size increase, the reconstructions should be performed over subset regions of interest, or a larger format (such as 2048 x 2048) would be required to obtain full resolution of the detail.

The CG result suggests that a more elaborate test phantom that can be dynamically balanced be tested with the developed algorithms. Also, a phantom which is tapered or segmented to simulate more realistic turbine blade parts should be tried. It is recommended that the system used for CT CG measurement support 360° scans, have the capability for spatially indexing the part to the CT coordinate system and have good positional repeatability of the mechanical aspects of the system. It is necessary to have the system well characterized for all physical and CT characteristics such as slice thickness and spatial resolution uniformity across the field of reconstruction.

7.0 REFERENCES

1. R. H. Bossi, R. J. Kruse and B. W. Knutson, "Computed Tomography of Electronics", WRDC-TR-89-4112, December 1989.

2. R. H. Bossi, J. L. Cline and B. W. Knutson, "Computed Tomography of Thermal Batteries and Other Closed Systems", WRDC-TR-89-4113, December 1989.

3. R. H. Bossi, J. L. Cline, E. G. Costello and B. W. Knutson, "X-Ray Computed Tomography of Castings", WRDC-TR-89-4138, March 1990.

4. R. H. Bossi, K. K. Cooprider, and G. E. Georgeson, X-Ray Computed Tomography of Composites", WRDC-TR-90-4014, July 1990.

5. P. Burstein and R. H. Bossi, "A Guide to Computed Tomography System Specifications", WRDC-TR-90-4026, August 1990.

6. R. H. Bossi and R. J. Kruse, "X-ray Tomographic Inspection of Printed Wiring Assemblies and Electrical Components", WRDC-TR-90-4091, October 1990.

7. G. E. Georgeson and R. H. Bossi and "X-Ray Computed Tomography of Full-Scale Castings," WL-TR-91-4049, October, 1991.

8. R. H. Bossi and G. E. Georgeson, "Computed Tomography Analysis of Castings" WL-TR-91-4121, January 1992.

9. "Nondestructive Evaluation Integrated Data Reduction Systems," Boeing Aerospace, D180-31159-1 (1988).

10. K. Hoang and G. Norman, "Baseline Survey of Computer Industrial Tomographic Inspection and Analysis on Four Representative Workloads form OC-ALC", September 21, 1988.

APPENDIX A - RADIOGRAPHIC IMAGING TECHNIQUES

The three basic techniques of radiographic imaging used in the CTAD program are film radiography, digital radiography, and computed tomography.

A1 Film Radiography

Conventional film radiography, as illustrated in Figure A1-1, uses a two-dimensional radiographic film to record the attenuation of the X-ray radiation passing through a three-dimensional object. This results in a shadowgraph containing the superposition of all of the object features in the image and often requires a skilled radiographer to interpret. The sensitivity in the image is determined by the attenuation coefficient for the material at the effective energy of the radiation beam, response of the X-ray film, film resolution, X-ray source spot size, and source-to-object-to-detector geometry. For objects which vary in thickness and material, the appropriate X-ray exposure will vary and can only be compensated for by multiple exposures at different energies or times, or as is commonly used, multiple film loads of variable sensitivity radiographic films.

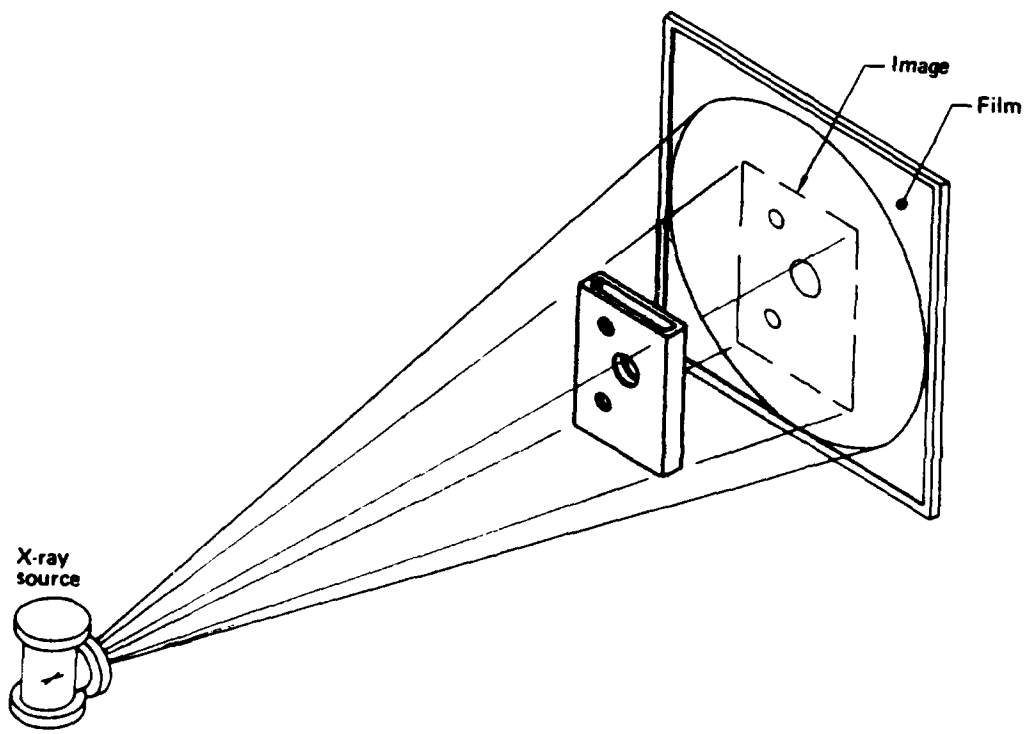

Figure A1-1 Film radiography.

A2 Digital Radiography

Digital radiography (DR) is similar to conventional film radiography. The DR is performed on a system where the film is replaced by a linear array of detectors and the X-ray beam is collimated into a fan beam as shown in Figure A2-1. The object is moved perpendicular to the detector array, and the attenuated radiation is digitally sampled by the detectors. The data are 'stacked' up in a computer memory and displayed as an image. The sensitivity is determined by the geometric factors, and the resolution, signal to noise and dynamic range of the detector array. Usually DR images have a sufficiently large dynamic range that allows a wide range of thickness and materials in an object to be imaged at suitable signal to noise with one scan.

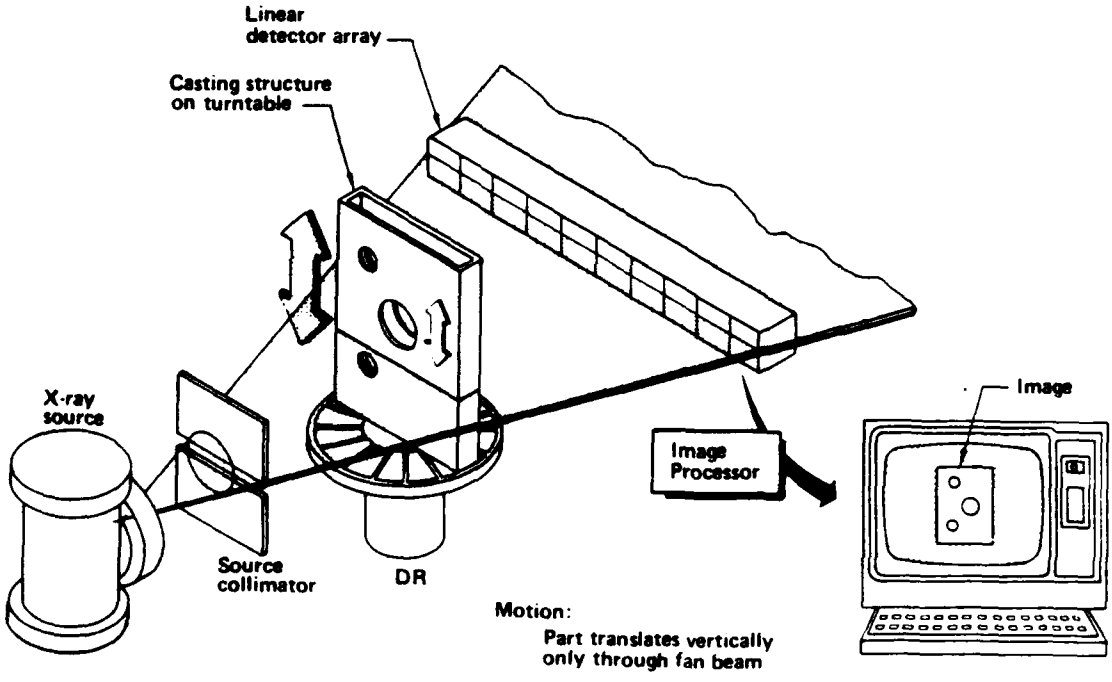

Figure A2-1 Digital radiography.

A3 Computed Tomography

Computed tomography (CT) uses X-ray transmission information from numerous angles about an object to computer reconstruct cross sectional images (i.e., slices) of the interior structure. To generate a CT image, X-ray transmission is measured by an array of detectors. Data are obtained by translating and rotating the object so that many viewing angles about the object are used. A computer mathematically reconstructs the cross-sectional image from the multiple view data collected. A primary benefit of CT is that features are not superimposed in the image, thus making it easier to interpret than radiographic projection images. The image data points are small volumetric measurements directly related to the X-ray attenuation coefficient of the material present in the volume elements defined by the slice thickness and the horizontal resolution capability of the CT system. The values and locations provide quantitative data for dimensional and material density/constituent measurements.

A3.1 Conventional CT

Conventional CT is shown in Figure A3-1. The X-ray beam is collimated to a narrow slit and aligned with a detector array to define a CT slice plane in the component. The slit collimation reduces scatter and improves the signal to noise in the image. For 100 percent coverage, multiple, contiguous slices must be taken over the entire component.

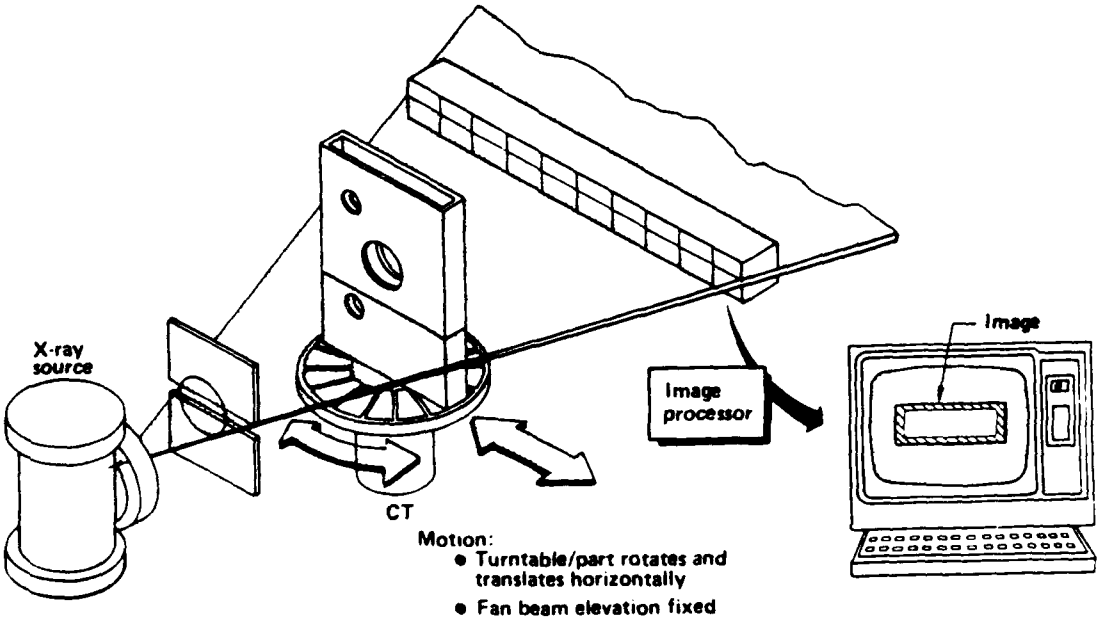

Figure A3-1 Computed tomography.

A3.2 Cone Beam CT

Cone beam CT is fundamentally the same as conventional CT; however, instead of collimating to a thin slice of radiation and using a linear detector array, an entire cone of radiation is used with an area array detector, as shown in Figure A3-2. The data acquisition in each angular view includes information for multiple CT slices along the object axis. The object will be rotated for data acquisition of multiple views. The data handling and reconstruction for cone beam CT is substantially more complicated than conventional CT, and a suitable display mechanism for viewing multiple plane images from the volumetric data set is needed. The advantage of the technique is that an entire volume can be scanned much more rapidly than is possible using conventional CT and taking scans at multiple axial positions. This offers a substantial cost savings for CT examinations of entire volumes. However, the scatter is increased and thus the signal to noise in the image is normally not as good as with conventional CT.

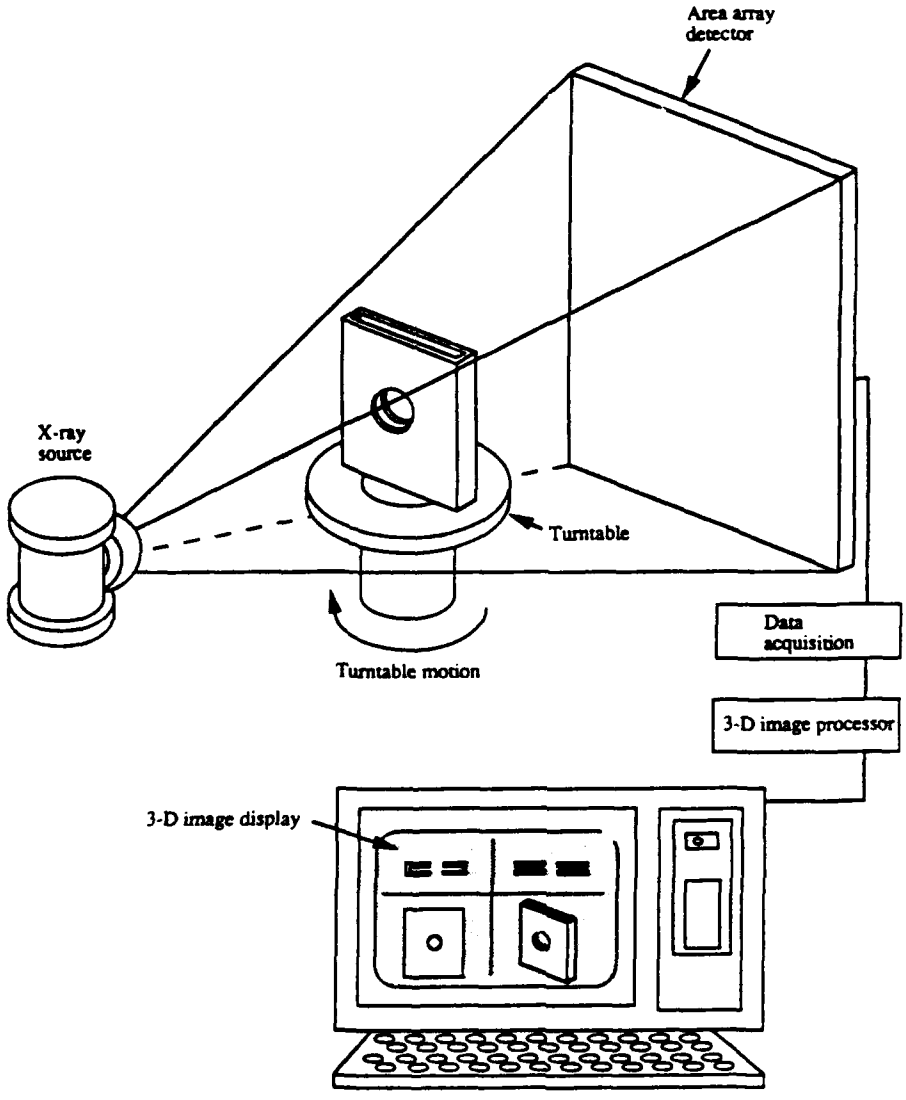

Figure A3-2 Cone beam CT.

APPENDIX B - CT PHANTOMS

A set of CT phantoms was developed for the CTAD program in order to provide consistent evaluation of results from various CT systems. The phantoms serve several purposes. First, they provide a quantitative measure of the CT system capability that can be used repetitively to assure consistent performance. Second, the quantitative measurements can be used in conjunction with part images to assess a quality level necessary to achieve desired detection or measurement levels in the inspected parts. Third, the phantoms can be used to select CT systems based on the desired sensitivity level for the CT application.

The use of phantoms for CT is complicated due to the wide range of parameters in any CT inspection. Therefore, caution must be used in extrapolating phantom data to suggest a "best" overall CT system. In fact, CT systems have varying designs that result in a range of performance characteristics. The phantoms allow the user a quantitative measure of quality level that, combined with other operating parameters, may suggest an optimum system. While the phantoms used in this program measure line pair resolution and contrast sensitivity, there are several other important parameters a user must be concerned with in selecting a CT system for scanning: scan time, field of view, object penetration, data manipulation, system availability and cost.

The CT performance phantoms are: line pair resolution phantom and contrast sensitivity phantom.

B1 Resolution Phantom

Figure B1-1 shows the line pair resolution phantom. The phantom consists of sets of metallic and acrylic plates of specified thickness. Line pairs of 0.5, 1, 2 and 4 lp/mm are formed by the phantom.

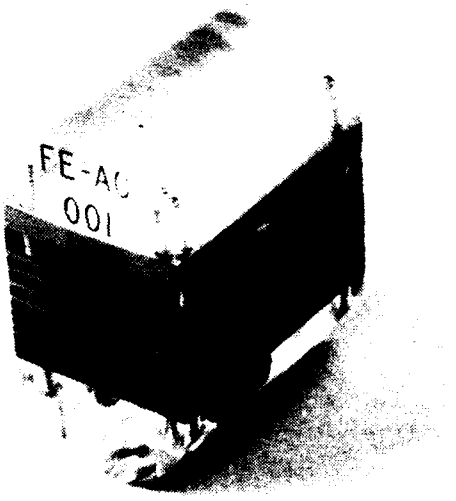

Figure B1-1 Photograph of the line pair resolution phantom.

The entire assembly is bolted together and the line pair plates can be changed if additional or a different range of line pairs is desired. Following CT scanning the reconstructed image is analyzed by measuring the modulation of the CT numbers resulting from a trace across the line pairs. The modulation at each line pair set is measured as a percentage, where the modulation measured between the 3 mm (0.12 in) thick metal and 3 mm (0.12 in) thick acrylic steps is 100 percent. Operating parameters such as field of view, slice thickness, integration time and detector collimation will affect the results. It is desirable to obtain data at CT system parameters that are the same as that used for part scanning. The resolution phantom has been fabricated in two forms, steel/acrylic and aluminum/acrylic. The steel/acrylic phantom is for systems of 300 kV and up, the aluminum/acrylic phantom is for systems under 300 kV.

Figure B1-2 shows a CT image of the steel resolution phantom obtained from a high-resolution CT system. The CT image density contour line across the gauge indicates modulation for the respective line pair measurements at approximately 82 percent at 1/2 lp/mm, 46 percent at 1 lp/mm, 4 percent at 2 lp/mm, and 0 percent at 4 lp/mm.

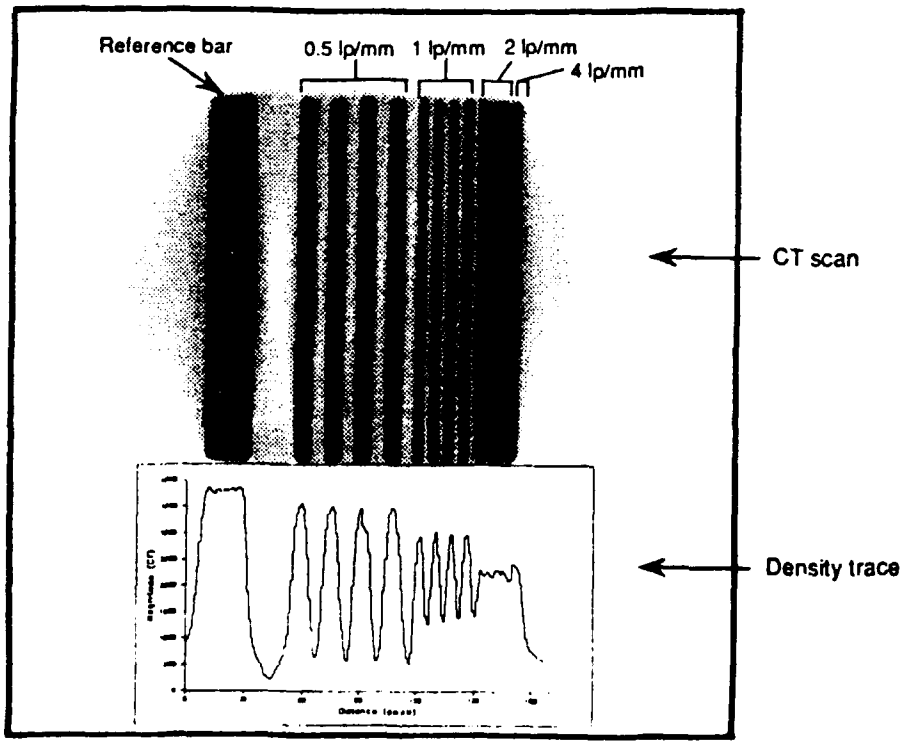

Figure B1-2 CT image of the line pair resolution phantom.

B2 Contrast Sensitivity Phantom

The contrast sensitivity phantom is a uniform disc of aluminum, 25 mm (1 inch) thick. Two sizes were made, one is 140 mm (5.5 inch) in diameter and the other is 70 mm (2.76 inch) in diameter. The smaller diameter size is used on systems with small fields of view or low kV. Figure B2-1 shows an example CT slice of the large aluminum contrast sensitivity phantom with the corresponding density trace.

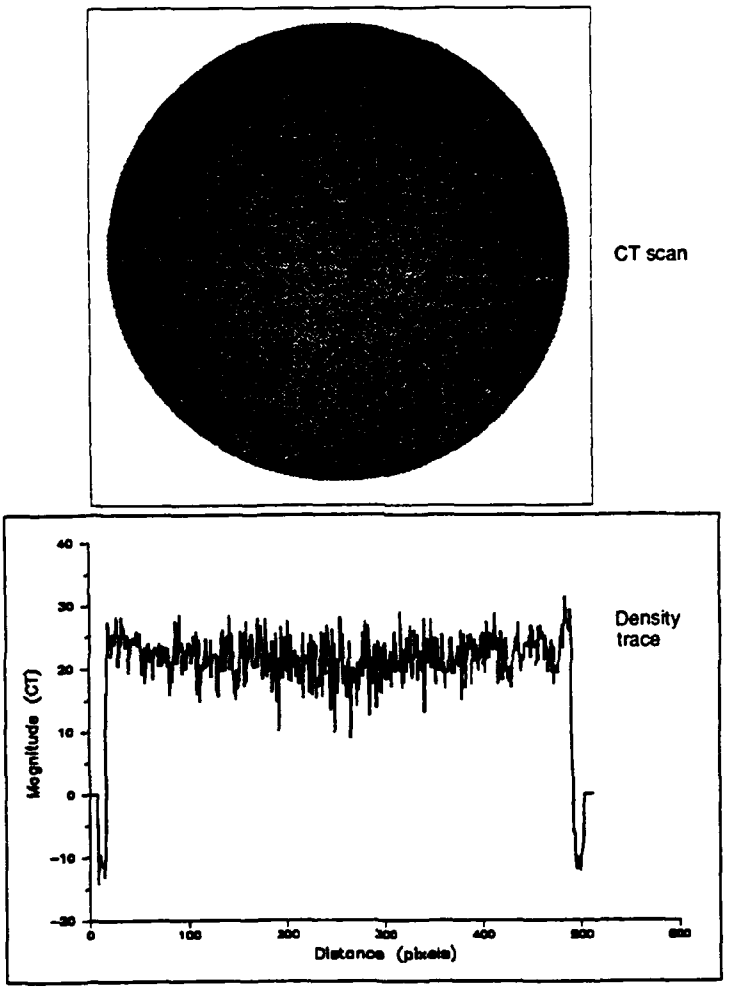

Figure B2-1 CT image of the contrast sensitivity phantom.

The measurement of contrast sensitivity is obtained by taking a region in the reconstructed image and determining the average and standard deviation for all CT numbers in the region. A typical region size of 1 cm (0.39 inch) diameter is used. Readings are usually taken at the center of the disk. The ratio of the average to the standard deviation is used as a signal to noise measurement. The inverse is a measure of contrast sensitivity. The signal to noise measurement for the image shown in Figure B2-1 is approximately 6.

The signal-to-noise ratio measurements are an important measure of system performance. The values improve with higher signal strengths. They also improve with smoothing algorithms in the reconstruction; however, this will decrease the resolution. Thus, the signal to noise and resolution must be considered together in assessing a quality level for performance.